Geoderma 154 (2010) 418–437

Contents lists available at ScienceDirect

Geoderma

journal homepage: www.elsevier.com/locate/geoderma

Soil mineralogy trends in California landscapes

R.C. Graham [a,*], A.T. O'Geen [b]

[a] Soil & Water Sciences Program, Department of Environmental Sciences, University of California, Riverside, CA 92521-0424, United States
[b] Department of Land, Air, and Water Resources, University of California, Davis, CA 95616, United States

ARTICLE INFO

Article history:
Received 17 August 2008
Received in revised form 12 May 2009
Accepted 18 May 2009
Available online 26 June 2009

Keywords:
Mineral weathering
Toposequence
Chronosequence
Climosequence
Lithosequence

ABSTRACT

California's diverse environmental gradients serve as natural experiments for examining controls on soil mineral distribution in landscapes. In this paper we use example soilscapes from throughout California to examine how lithology, climate, topography, and duration of pedogenesis interact to produce distinctive weathering environments and characteristic suites of soil minerals. Seven soil-geomorphic sequences were assembled from the literature to illustrate major soil mineralogical trends: 1) granitic terrain of the Peninsular Ranges, 2) granitic terrain of the central Sierra Nevada, 3) andesitic terrain of the northern Sierra Nevada, 4) fluvial terraces on the east side of the Great Valley, 5) marine terraces of the central coast, 6) ultramafic terrain of the Klamath Mountains, and 7) an alluvial fan in the Mojave Desert. Results of this analysis show that kaolin is present in virtually all pedons, irrespective of climate, parent material, age, or topographic position. Kaolin does not form in ultramafic soils due to insufficient aluminum. Many secondary clay minerals reflect the state's strong climatic influence, with palygorskite, smectite, and vermiculite in the dry, hot environments; hydroxy-interlayered minerals, gibbsite, and short range-ordered minerals in the cool, moist environments. In arid and semi-arid regions, the distribution of calcite, gypsum, and soluble salts is strongly related to patterns of eolian dust deposition and water infiltration and leaching.

1. Introduction

The diverse geologic, topographic, and climatic settings within the state of California create distinct landscapes with highly contrasting pedogenic processes. The resulting wide variety of soils and soil minerals plays a critical role in ecosystem function, land management, and quality of life. Inherent soil fertility issues are often directly linked to soil mineralogy (e.g., Page et al., 1967; Murashkina et al., 2007). Soil water behavior and irrigation management, so critical in arid and semi-arid California, are controlled to a large degree by the amount and kind of soil clays (Frenkel et al., 1978). Soil aggregation and carbon sequestration potential vary with mineralogy (Rasmussen et al., 2005). Many water quality issues begin with soil erosion, which is controlled in part by soil mineralogy (Le Bissonnais and Singer, 1993). Eroded soil particles can carry with them adsorbed pesticides and other agricultural chemicals (Agassi et al., 1995). Wind erosion, generated from such sources as agricultural operations, off-highway vehicle use, and dry lakebeds, causes health hazards due to inhalation of fine mineral particulates (Baker et al., 2005; Reheis, 2006). The amount and kind of soil clays determine slope stability (Moody, 1989). Soil minerals can be used to help understand the current behavior of wetlands (O'Geen et al., 2008) and aridlands (Reid et al., 1993), interpret paleoenvironmental conditions (Amundson et al., 1989), and assist in forensic investigations (Stam, 2004).

In order to address society's needs related to soil resources, it is important to understand the landscape distribution of soil minerals and the processes responsible for their occurrence. The gradients between environmental extremes in California provide effective natural experiments for determining the controls on soil mineral distribution. In this paper we use example soilscapes from throughout California to examine how lithology, climate, topography, and duration of pedogenesis interact to produce distinctive weathering environments and characteristic suites of soil minerals. The relevance of this understanding extends beyond the state, because analogous environments and soil-related issues are found worldwide.

2. Environmental setting

California is divided into eleven physiographic provinces (Fig. 1). Each of these regions exhibits distinctive natural features of geology, topography, climate, and vegetation assemblages. In the broader view of plate tectonics, most of California is on the North American plate, but its western margin is positioned across the boundary with the Pacific plate (Norris and Webb, 1990). As a result of the plate movements, sediments have been accreted onto the western margin of the continent so that much of coastal California consists of sedimentary or metasedimentary rocks (Fig. 2). Amid these accreted sediments are patchy intrusions of ultramafic rocks (peridotites and serpentinites) derived from mantle material. Metamorphic rocks cap the granitic batholith throughout the low- and mid-elevations of the northern Sierra Nevada. Much of this covering has been removed by erosion at

* Corresponding author.
E-mail address: robert.graham@ucr.edu (R.C. Graham).

0016-7061/$ – see front matter
doi:10.1016/j.geoderma.2009.05.018

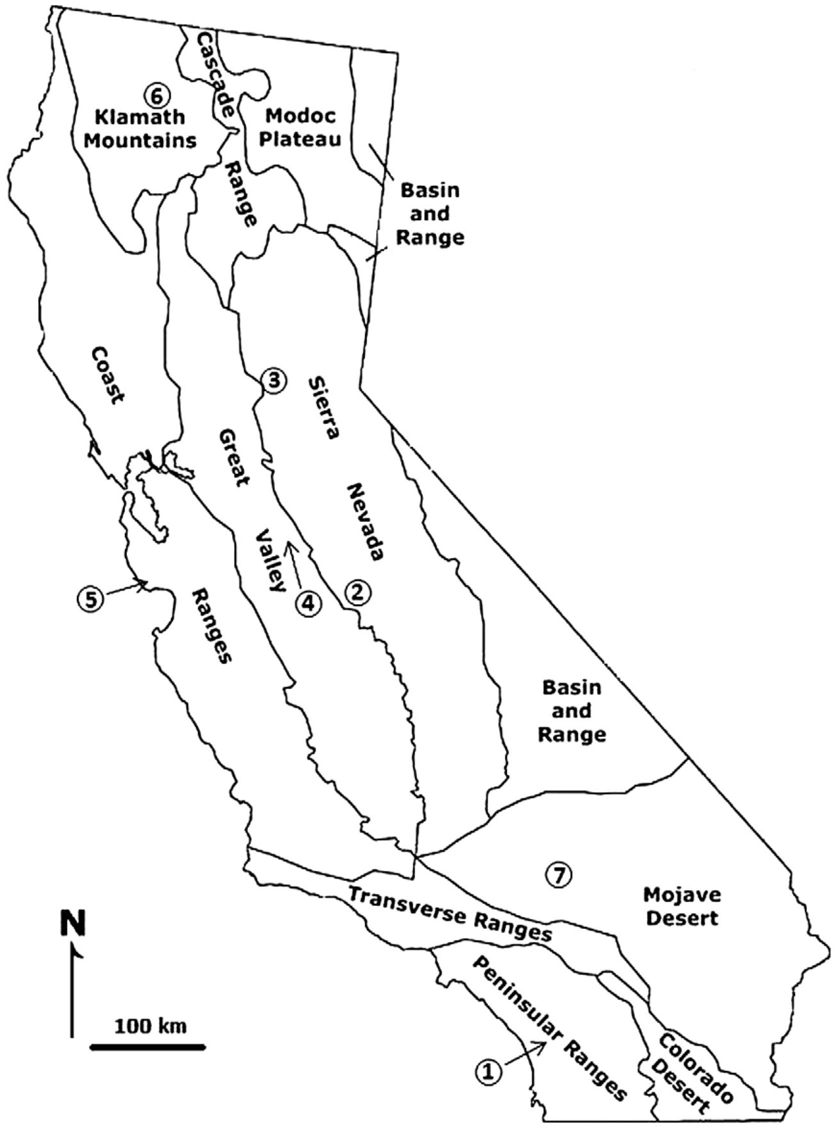

Fig. 1. Physiographic regions of California (map source: U.S. Geological Survey). Locations of the soil mineralogy — landscape examples highlighted in this review are indicated: (1) granitic terrain of the Peninsular Ranges, (2) granitic terrain of the central Sierra Nevada, (3) andesitic terrain of the northern Sierra Nevada, (4) fluvial terraces on the east side of the Great Valley, (5) marine terraces of the central coast, (6) ultramafic terrain of the Klamath Mountains, and (7) alluvial fan in the Mojave Desert.

high elevations and to the south, where uplift has been more extensive. Granitic rock comprises about 20% of the state's land area, primarily in the Sierra Nevada, but also in the Transverse and Peninsular Ranges of southern California, and scattered throughout the Mojave Desert, Basin and Range, Klamath Mountains, and the central Coast Ranges. Volcanic deposits are concentrated in the Cascade Range and Modoc Plateau, but also are scattered throughout the Mojave Desert, Basin and Range, and, to a lesser extent, the Sierra Nevada and Coast Ranges. The long geosynclinal trough of the Great Valley contains a vast expanse of Holocene alluvium, but older alluvial terraces remain in places along its margins. Alluvium is also abundant in intermontane valleys and basins bounded by faults in southern and eastern regions. High elevations, mostly in the Sierra Nevada, were subjected to extensive alpine glaciation during the Pleistocene, so glacial deposits are present in those regions and the valleys that lead down from them.

California is subject to a variety of climatic conditions originating from marine, topographic, and latitudinal influences. Generally, precipitation-bearing storms move down from the north and west from the Pacific Ocean during the winter, associated with extratropical cyclones and associated troughs of the jet stream (Minnich, 2007). Since the jet stream tends to be positioned off the coast of the Pacific Northwest extending to northern California, more storms reach the northern part of the state and storm frequency decreases with increasing distance to the south (Minnich, 2007). As a result, mean annual precipitation decreases toward the south (Fig. 3). At any given latitude, rainfall is relatively high along the coast, increases with elevation in coastal mountains and then decreases in rain shadows to the east. The highest mean annual precipitation occurs in the north coastal mountains, which receive over 2750 mm, mostly as rain. Precipitation increases dramatically as the storms pass over the high elevations of the Sierra Nevada. At lower elevations the precipitation is dominantly rain, whereas several meters of snow fall annually at the higher elevations. The southeastern deserts have particularly low mean annual precipitation, less than 50 mm in Death Valley and the Imperial Valley. Limited summer precipitation is occasionally delivered to some parts of southern and southeastern California by monsoonal weather patterns.

Mean annual temperatures vary as a result of latitude and position of the jet stream (Fig. 4). Coastal regions remain cool in summer and mild in winter due to the exchange of heat between tropical and polar latitudes by the California Current and associated air mass (Miller and

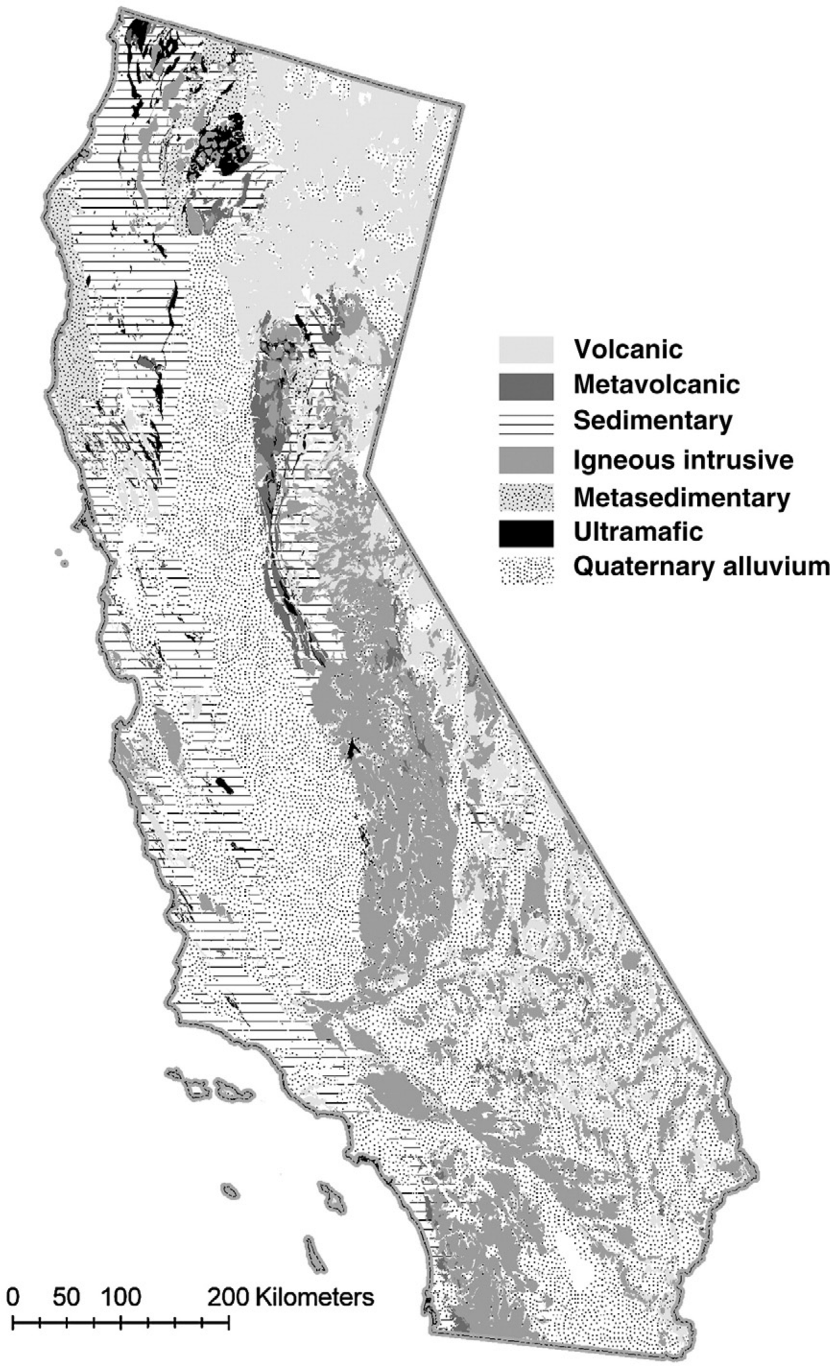

Fig. 2. Generalized geologic map of California. California Department of Conservation, Division of Mines and Geology. Map scale 1:750,000.

Hyslop, 2000). Onshore winds maintain cool conditions in the summer in the Coast Ranges within 100 km of the coast. Temperatures increase substantially in the inland valleys (Fig. 4). At mean sea level, January temperatures are approximately 5 °C warmer in southern California compared to northern California. Most coastal valleys and the Great Valley have a frost-free season of 225 to 300 days. Temperatures decrease dramatically with increasing elevation. The average frost free period is less than 100 days above 1500 m in the Modoc Plateau, Sierra Nevada, and Transverse Ranges (Minnich, 2007). In desert regions, mean air temperatures range from 7 to 11 °C in January and 24 to 38 °C in July (Western Regional Climate Center, accessed 2008).

Nine of the 12 soil orders from the USDA soil taxonomic system (Soil Survey Staff, 2006) are sufficiently abundant to be displayed at the scale depicted in Fig. 5. Entisols and Aridisols cover most of the desert regions, Basin and Range, and the southern Great Valley. Mollisols are common on the Modoc Plateau, the Coast Ranges, the Transverse Ranges, and the Great Valley. Alfisols are prevalent in the semi-arid, mid- to low-elevation mountains and on alluvial terraces. Inceptisols and Entisols are common in mountainous terrain and on Holocene and late Pleistocene alluvial deposits. Ultisols are found in the mid-elevations of the northern Sierra Nevada, Klamath Mountains, and northern Coast Ranges. Andisols are predominantly in the Cascade Range and Modoc Plateau. Vertisols are scattered over much of the state, but are concentrated in the Great Valley, the Modoc Plateau, the Peninsular Ranges, and the southern Coast Ranges. Histosols predominate in the Sacramento Delta region of the Great Valley, but also are

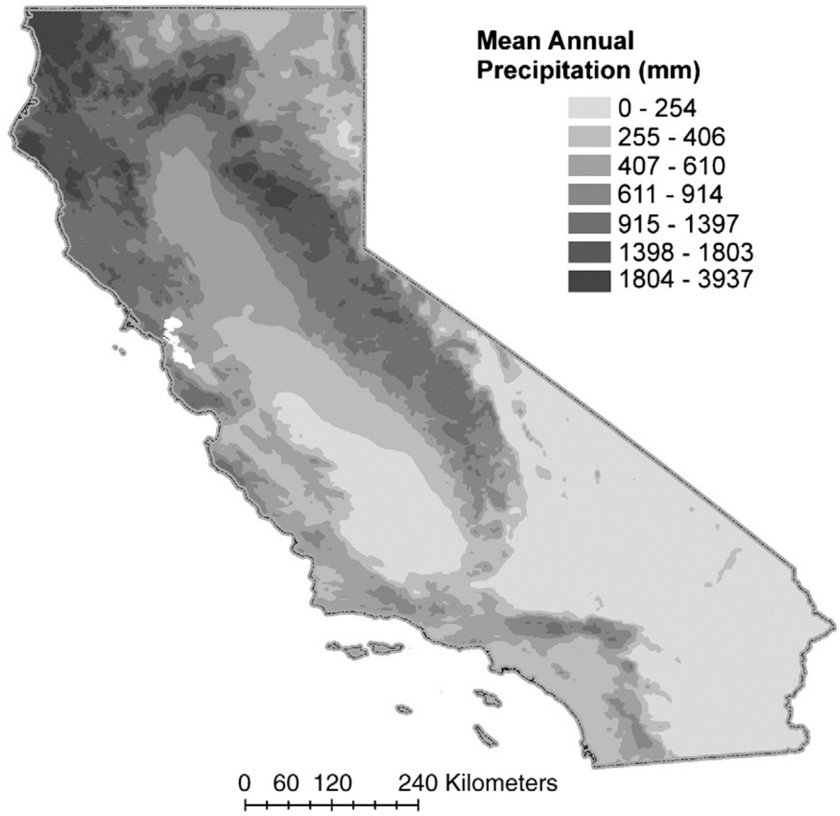

Fig. 3. Distribution of mean annual precipitation in California. USDA-NRCS PRISM dataset mapped at a horizontal resolution of 800 m.

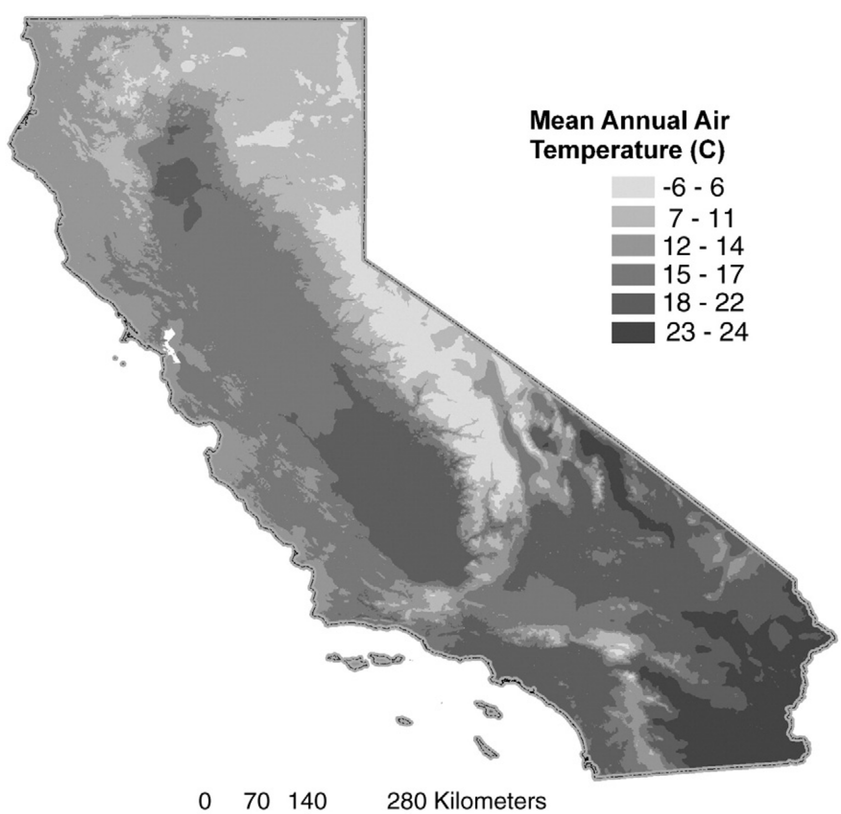

Fig. 4. Distribution of mean annual temperature in California. USDA-NRCS PRISM dataset mapped at a horizontal resolution of 800 m.

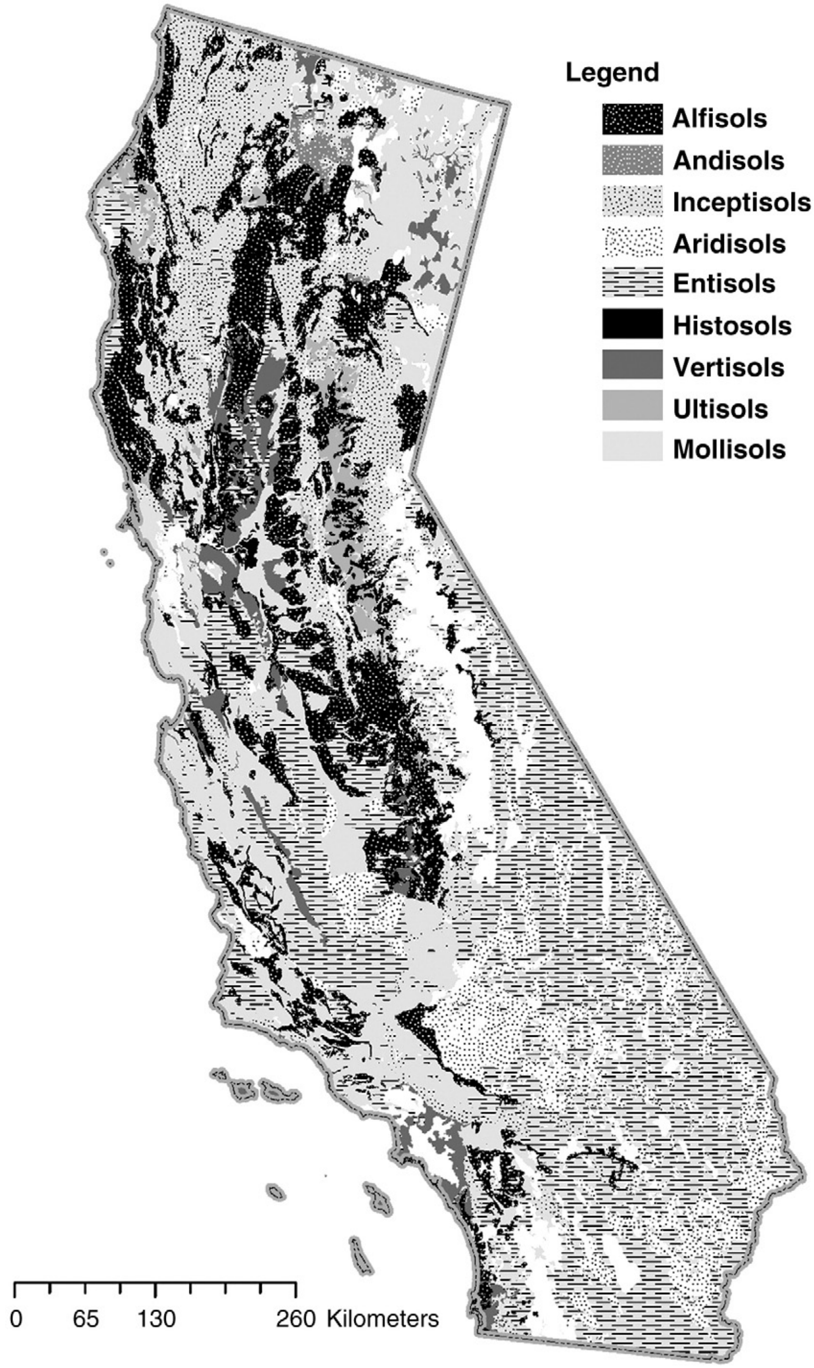

Fig. 5. Distribution of soil orders in California. The spatial extent of regions containing Oxisols and Spodosols was small and impossible to depict at this scale. Gelisols have not been identified in California. USDA-NRCS STATSGO Database. Map scale 1:250,000.

present in localized wet areas of mountain meadows. Spodosols and Oxisols occur in areas too small to show on the map in Fig. 5. Gelisols apparently have not been found, but may be present on some high elevation north-facing slopes.

3. Soil mineralogy — landscape relationships

Seven examples of soil mineralogy–landscape relationships throughout the state (Fig. 1) are presented here. The sources of the data are mostly from published work, but in some cases they are based on unpublished reports or dissertations. All sources are cited. We note that some of the studies were done several decades ago using soil morphological designations that have been superseded. We have converted those designations to ones that are currently used (Soil Survey Staff, 2006).

3.1. Granitic terrain of the Peninsular Ranges

The Peninsular Ranges in southwestern California are dominated by tonalite (quartz diorite), a granitic rock of intermediate composition. While some peaks in these ranges exceed 2700 m, much of the landscape has less relief, with rolling uplands and hills interspersed with alluvial valleys at elevations ranging from 150 to 500 m. The soils of this region have a xeric moisture regime and thermic temperature regime. This region has been renowned for its agricultural production, particularly citrus and avocados. It is also a heavily populated region that continues to experience suburban development.

Soil mineralogical trends in this region are well represented by a toposequence study in San Diego County (Nettleton et al., 1968, 1970). The toposequence extended from upper slopes (smooth hilltops, upper

Fig. 6. Landscape in Peninsular Ranges granitic terrain (Fig. 1) (photo credit: P. Sternberg).

backslopes) through middle and lower backslopes to footslopes, encompassing an elevation difference of 18 m across a horizontal distance of about 150 m. A similar landscape is shown in Fig. 6. The soils on the footslopes are formed in alluvium of variable thickness, while the upland soils are formed in residuum or colluvium over residuum. The mean annual precipitation at the site is 380 mm, occurring as rain in late fall through early spring. The upper slope soils formed under chaparral shrubs while the lower slope soils formed under grassland with scattered California live oaks (*Quercus agrifolia*). The tonalite underlying the toposequence is composed of 56% andesine (An_{43}), 8% orthoclase, 9% quartz, 14% biotite, and 13% hornblende.

Some of the properties of three of the soils along the toposequence are presented in Table 1. Soils on the upper slopes are in the Vista series (coarse-loamy, mixed, superactive, thermic Typic Haploxerepts). Fallbrook soils (fine-loamy, mixed, superactive, thermic Typic Haploxeralfs) are on the middle and lower backslopes, and soils of the Bonsall series (fine, smectitic, thermic Natric Palexeralfs) are on the footslopes The Vista and Fallbrook soils formed primarily in tonalite residuum, whereas the Bonsall soils formed in pedisediments as well as the underlying weathered tonalite. The tonalite bedrock underlying the soils has weathered such that it is friable and can be crushed by hand and excavated with some difficulty using a spade. This weathered bedrock has 10 YR hues, as do the soils on the upper slopes. These hues are suggestive of goethite (Schwertmann, 1993). Soils on the middle and lower backslopes have much redder (5 YR hues) B horizons, while those on the footslopes have mostly 7.5 YR hues. Although pedogenic Fe oxides are not particularly abundant (≤16 g/kg), presumably there is sufficient hematite to impart the reddish hues via grain coatings in these

Table 1
Properties of soils in a toposequence on granitic terrain in the Peninsular Ranges (Nettleton et al., 1968).

Horizon	Depth (cm)	Dry color	Texture[a]	Sand (%)	Silt (%)	Clay (%)	O.C. (g kg^{-1})	pH (1:1)	$CEC_{8.2}$ (cmol kg^{-1})	Fe_d (g kg^{-1})	Clay mineralogy[b]
Upper slopes: Vista series (coarse-loamy, mixed, superactive, thermic Typic Haploxerept)											
A1	0–7.5	10 YR 4/2	COSL	73	17	10	9.6	6.9	17	10	M4 K2 HBt
A2	7.5–23	10 YR 4/3	COSL	71	18	11	5.6	6.6	19	9	V3 K2 HB1
A3	23–48	10 YR 4/3	COSL	70	18	12	3.4	6.8	20	10	V3 K2 HB1
Bw1	48–71	10 YR 4/3	COSL	69	19	12	2.8	6.7	19	9	V3 K2 HB1
Bw2	71–89	10 YR 5/4	COSL	71	18	11	1.0	6.9	23	11	K3 V2 HB1 Mt
Cr1	89–112	10 YR 5/4	ROCK	82	13	5	0.3	7.1	15	7	V4 K2 HBt
Cr2	112–155	10 YR 5/3	ROCK	83	12	5	0.3	7.4	16	8	V4 K2 HBt
Middle and lower backslopes: Fallbrook series (fine-loamy, mixed, superactive, thermic Typic Haploxeralf)											
A1	0–5	10 YR 5/3	SL	73	19	8	7.3	6.6	10	8	M4 K2 HBt
A2	5–15	10 YR 5/3	SL	72	20	8	5.0	6.5	9	7	M4 K2
AB	15–30	5 YR 5/3	L	66	21	13	3.0	6.8	11	7	HB4 K2 M1
Bt	30–71	5 YR 5/4	SCL	53	18	29	2.6	6.9	19	14	K3 HB2 M2 V1
BC	71–119	5 YR 6/4	L	72	13	15	0.7	7.4	19	9	K4 M2 Vt HBt
Cr	119–173	2.5 YR 4/4	ROCK	80	11	9	0.2	7.6	17	7	K3 M2 V1 HBt
Footslopes: Bonsall series (fine, smectitic, thermic Natric Palexeralfs)											
A1	0–15	10 YR 5/3	SL	68	23	9	7.0	6.6	9	7	M4 K2 Vt HBt
A2	15–25	10 YR 5/3	SL	63	25	12	2.8	6.8	10	8	HB2 K2 Sm2 Vt
Bw	25–36	7.5 YR 5/4	CL	42	19	39	4.7	6.8	26	16	K3 Sm2 V1 Mt HBt
Bt	36–69	10 YR 5/4	C	41	21	38	2.1	8.0	25	10	Sm3 K3 Vt Mt HBt
Btkn	69–97	10 YR 6/4	C	48	23	29	1.1	8.1	27	9	nr
BCn1	97–122	7.5, 2.5 YR 5/4	SL	64	17	19	0.2	8.0	23	13	Sm3 K2 Mt HBt
BCn2	122–152	7.5 YR 4/4	SL	70	11	19	0.2	8.0	20	12	nr
CBn	152–226	7.5 YR 6/4	SCL	52	27	21	0.2	8.0	25	12	Sm3 K2 Mt HBt
2Cr1	226–279	10 YR 8/3	ROCK	57	29	14	<0.1	8.3	37	14	nr
2Cr2	279–305	2.5 Y 7–8/4	ROCK	51	33	17	<0.1	8.1	31	13	Sm3 K2 M1 HBt

[a] C = clay, CL = clay loam, COSL = coarse sandy loam, L = loam, ROCK = rock fabric, SCL = sandy clay loam, SL = sandy loam.
[b] HB = hydrobiotite, K = kaolin, M = mica, Sm = smectite, V = vermiculite; t = trace, 1 = minor amount, 2 = moderate amount, 3 = major amount, 4 = dominant; nr = not reported.

coarse-textured soils. Maximum clay content increases downslope, ranging from 12% in the Bw1 horizon of the Vista soil to 38% in the Bt horizon of the Bonsall soil. Organic carbon content is <10 g kg^{-1} in the A horizons and decreases with depth. Soil pH generally increases with depth and the maximum pH increases downslope, from a high of 7.4 in the Vista soil to a high of 8.3 in the Bonsall soil. The upper and middle slope soils (Vista and Fallbrook) do not contain calcium carbonate or appreciable exchangeable Na, but the footslope soils (Bonsall) contain a few percent calcium carbonate and exchangeable sodium percentages up to 20 in subsoil horizons (data not shown). The Na on the exchange and the Ca in $CaCO_3$ are derived from the weathering of andesine. These weathering products are leached from upper slope soils to the Bonsall soils on lower slopes where they are incompletely removed because the clayey subsoil textures there impede leaching. Amorphous silica accumulates in the Bonsall subsoil for the same reasons (data not shown).

The initiation of soil formation in this landscape hinges upon a simple mineralogical transformation; that is, the transformation of biotite to vermiculite. This transformation involves replacement of interlayer K with hydrated, exchangeable Mg and the release and oxidation of octahedrally coordinated Fe. The transformation increases the volume of the micaceous grains, since the d_{001} spacing of biotite is 1.0 nm, while that of vermiculite is 1.4 nm. The expansion of biotite produces many small cracks within the general rock fabric (Frazier and Graham, 2000), increasing its porosity from $<1\%$ to between 20 and 35%. This increase in porosity allows water to percolate easily through the rock material (Graham et al., 1997) and it greatly decreases its structural integrity (Clayton and Arnold, 1972; Jones and Graham, 1993). As a result the bedrock becomes much more susceptible to chemical weathering and to physical disruption by burrowing ground squirrels.

On the summit and backslope positions (Vista and Fallbrook soils), biotite weathers to vermiculite, hydrobiotite (regularly interstratified biotite/vermiculite), and kaolinite. These weathering reactions proceed throughout the profiles producing pseudomorphic replacements of the original biotite grains. It is the vermiculite in sand-size biotite pseudomorphs that gives such high CEC values to the Cr horizons, which have low clay contents. The biotite weathering products enter the clay fraction (Table 1) through physical disruption or dispersion of the pseudomorphs. In the Vista soils, which have relatively low clay contents, most of the weathering products remain in the silt- and sand-sized biotite pseudomorphs, again contributing to relatively high CEC values. Feldspar grains are only slightly weathered and do not have any associated weathering products. Hornblende appears unweathered.

Somewhat lower on the backslopes, Fallbrook soils are more intensely weathered, sola are thicker, and illuviation has contributed to an argillic horizon with nearly 30% clay. Weathering intensity is greater on these lower slope positions because of water flow from upslope and increased water retention in the finer textured soil material. Mineral components are the same as in the upslope Vista soils, but kaolin is more abundant in the clay fraction of the subsoil horizons. In situ weathering of vermiculite and disaggregation of biotite pseudomorphs contribute to the increased clay, and kaolin, content of the B horizons.

Soils on the footslopes (Bonsall soils) are wet for long periods of time as moisture accumulates via water flow from upslope. Not only do these soils receive soluble weathering products from upslope, but they are also intensely weathered due to their relatively high moisture status. The pedogenic environment is rich in silica, sodium, and magnesium, which favors smectite formation. Feldspars weather pseudomorphically to smectite and, although biotite weathering products are the same as in upslope soils, formation of kaolin is generally less favored in these more silica-rich soils. Hornblende weathering contributes to the formation of smectite and Fe oxides.

Notably, mica is a major component of the clay fraction in the surface horizon of all of the soils in the toposequence (Table 1). This mica has formed through a process involving the biocycling of K. Plants scavenge K from deeper within the soil, incorporate it into their biomass, and return it to the soil surface in litter. The K released by litter decomposition is then incorporated and fixed in the interlayer of vermiculite, transforming it back to a mica with a d_{001} spacing of 1.0 nm. This vermiculte-to-mica transformation is common in dryland soils of California (Nettleton et al., 1973) and occurred within 41 years in lysimeter soils in southern California (Tice et al., 1996).

3.2. Granitic terrain of the central Sierra Nevada

The Sierra Nevada is the dominant mountain range in California (Fig. 1). It is 640 km long and 65 to 160 km wide and reaches elevations exceeding 4250 m. In the central and southern parts of the range, multiple intrusions of granitic rock dominate the lithology (Norris and Webb, 1990). As a result of active tectonism, the Sierra Nevada as a whole is tilted so that the east-facing scarp is exceptionally steep, whereas the west side slopes comparatively gradually toward the Great Valley. The winter storms that deliver the bulk of the precipitation ($>75\%$) generally move in from the west and encounter the Sierra Nevada as an orographic barrier. As the moisture-laden air rises up the western slope, it cools and releases its moisture as rain at the lower elevations and as snow at the higher elevations (Hornbeck, 1983). Thus, the western slope of the Sierra Nevada presents an elevational transect along which temperature decreases and precipitation increases with increasing elevation. Changes in vegetation are coincident with the climatic changes such that the lower elevations support an oak savannah and successively higher elevations support characteristic conifer species. The western slope of the Sierra Nevada contains the key watersheds that provide water to the vast agricultural endeavors of the Great Valley as well as to major metropolitan areas. The forests have also contributed valuable timber resources.

Soil mineralogical trends along an elevational transect in the central Sierra Nevada (Fig. 1) have been documented by Dahlgren et al. (1997). The transect begins at an elevation of about 200 m and extends to 2865 m (Fig. 7). With increasing elevation the mean annual precipitation increases from 330 to 1270 mm. Above an elevation of 1594 m most of the precipitation falls as snow, while at lower elevations precipitation is as rain or snow that melts between storms. Soil temperature regimes progress through thermic, mesic, frigid, and cryic with increasing elevation. The soil moisture regime is dominantly xeric, but probably is udic above about 2100 m. Four distinct vegetation zones occur: oak woodlands (<1008 m), oak/mixed conifer forest (1008–1580 m), mixed conifer forest (1580–2626 m), and subalpine mixed-conifer forest (2626–3200 m). While the western slope of the Sierra is dissected by deep river canyons, the intervening ridges often present relatively subdued terrain. Soils in this transect were sampled within these landscapes on knoll-crest positions with 9 to 15% slopes to the south. All of the soils sampled are underlain by bedrock; granodiorite at the higher elevations (≥ 1390 m) and tonalite at the lower elevations.

Four of the seven soils that make up the elevational transect will be discussed here. The low elevation (198 m) soils are in the Vista series (coarse-loamy, mixed, superactive, thermic Typic Haploxerepts). They support annual grasses with an open oak woodland (Fig. 7a). Soils of the Musick series (fine-loamy, mixed, semiactive, mesic Ultic Haploxeralfs) are found at a mid-elevation (1390 m), but below the winter snowline. The vegetation here is dominated by ponderosa pine (*Pinus ponderosa*), incense cedar (*Calocedrus decurrens*), and California black oak (*Quercus kelloggii*). Soils at mid-elevation but above the winter snowline (1800 m) are in the Shaver series (coarse-loamy, mixed, superactive, mesic Humic Dystroxerepts). They support a mixed conifer forest with white fir (*Abies concolor*), sugar pine (*Pinus lambertiana*), ponderosa pine, and incense cedar (Fig. 7b). At the highest elevation along the transect (2865), the soils have not been assigned a series name, but will be referred to here as Cryepts (sandy-skeletal, mixed Typic Humicryepts). These soils support relatively open stands of lodgepole a

b

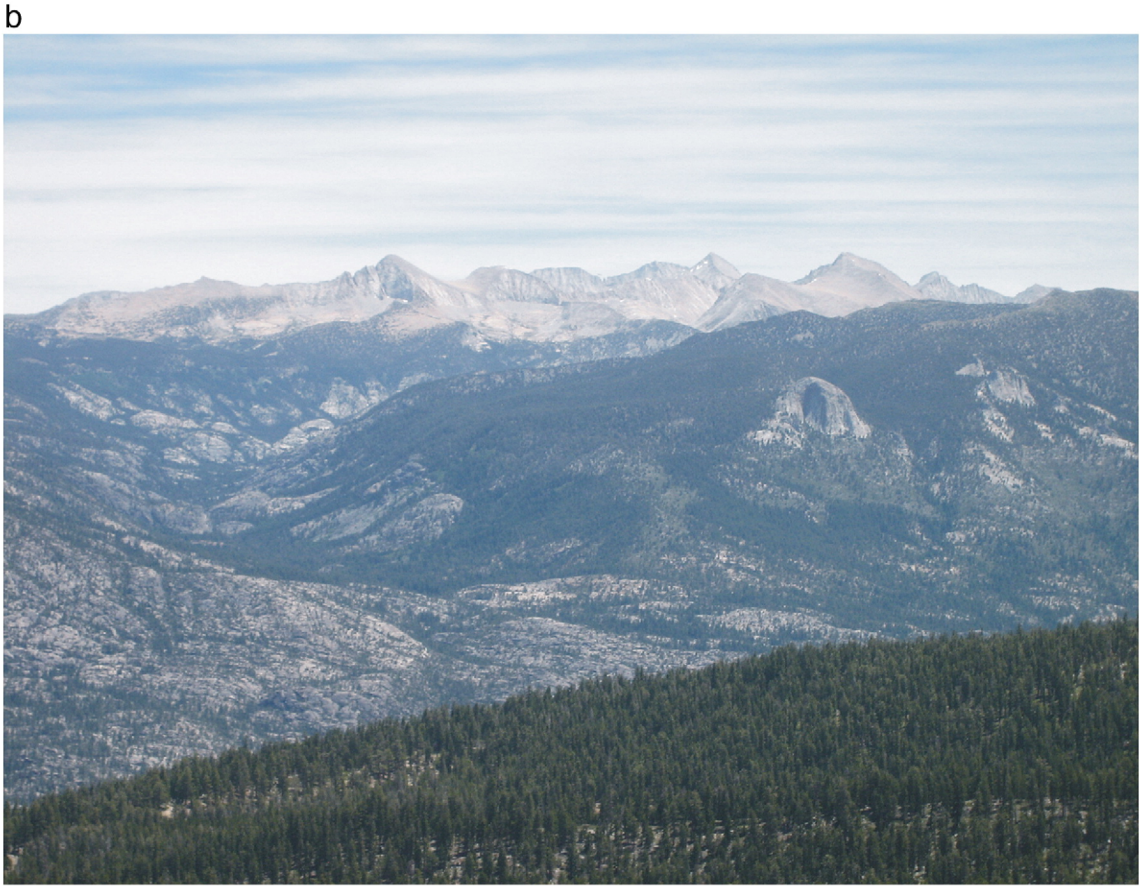

Fig. 7. Granitic terrain in the central Sierra Nevada (Fig. 1) showing (a) annual grasses and open oak woodland at an elevation of about 200 m and (b) mixed conifer forest at about 2200 m with high alpine peaks in the background (photo credit: R. Amundson).

pine (*Pinus contorta murrayana*) and western white pine (*Pinus monticola*).

Selected properties of the soils are presented in Table 2. At the highest elevation, soils are underlain by hard bedrock, but at all other elevations they are underlain by a zone of friable, weathered bedrock (Cr horizon). The soils and the weathered rock zone are relatively thin over hard bedrock at the lowest elevation, but at the mid-elevations soils are much thicker and Cr horizons, though not measured in this study, are often several meters thick. These zones of weathered granitic bedrock, formed by the same mechanisms described for the tonalite of the Peninsular Ranges, have substantial water-holding capacities and are critical to the survival of the forest ecosystems in this summer-dry region (Anderson et al., 1995; Hubbert et al., 2001; Rose et al., 2003; Witty et al., 2003).

Most of the soils in the elevational transect have 10 YR hues, indicative of goethite as the predominant iron oxide, but the Musick soils

Table 2
Properties of soils in an elevational transect on granitic residuum in the central Sierra Nevada (Dahlgren et al., 1997).

Horizon	Depth (cm)	Dry color	Texture[a]	Sand (%)	Silt (%)	Clay (%)	O.C. (g kg^{-1})	pH (1:1)	CEC_7 (cmol kg^{-1})	Fe_d (g kg^{-1})	Al_o (g kg^{-1})	Clay mineralogy[b]
198 m elevation: Vista series (coarse-loamy, mixed, superactive, thermic Typic Haploxeralf)												
A	0–14	10 YR 5/4	COSL	79	11	10	27	6.3	12	4	<1	M3 K2
Bw1	14–19	10 YR 6/3	LCOS	80	12	8	4	7.4	7	5	<1	nr
Bw2	19–34	10 YR 5/3	LCOS	79	13	8	3	7.3	7	5	<1	nr
Bt	34–56	10 YR 5/3	COSL	76	14	10	3	7.0	7	5	<1	M3 K2
Crt	56–71		ROCK									nr
R	71+		ROCK									
1390 m elevation: Musick series (fine-loamy, mixed, semiactive, mesic Ultic Haploxeralf)												
O	14–0											
AE	0–29	10 YR 6/3	SL	60	27	15	16	5.6	12	8	1	K3 M2 HIV1
EBt	29–38	10 YR 6/4	SL	62	24	16	8	5.8	9	9	<1	nr
Bt1	38–54	10 YR 5/8	SCL	64	14	27	3	5.2	9	14	<1	K3 M1 HIV1
Bt2	54–69	2.5 YR 5/6	SCL	63	16	25	2	5.1	8	12	<1	nr
BCt1	69–96	7.5 YR 6/8	SL	67	18	17	1	5.0	9	10	<1	nr
BCt2	96–180	7.5 YR 7/3	SL	76	17	11	1	5.0	8	7	<1	nr
Cr	180+		ROCK									
1800 m elevation: Shaver series (coarse-loamy, mixed, superactive, mesic Humic Dystroxerepts)												
O	4–0											
A1	0–4	10 YR 5/3	LS	80	15	5	39	6.2	18	4	6	HIV2 K2 M1 G1
A2	4–18	10 YR 5/3	LS	79	17	4	16	6.0	11	4	7	nr
A3	18–46	10 YR 5/3	LS	83	13	6	8	6.1	10	4	4	nr
A4	46–70	10 YR 5/3	LS	80	15	8	6	6.0	9	5	5	K3 HIV3
Bw1	70–102	10 YR 6/3	LS	80	15	8	5	5.9	9	4	4	nr
Bw2	102–172	10 YR 5/2	LS	83	13	6	1	5.7	5	4	<1	nr
Cr	172+		ROCK	85	12	3	1	5.7	6	4	<1	nr
2865 m elevation: Cryepts (sandy-skeletal, mixed Typic Humicryepts)												
O	3–0											
A1	0–6	10 YR 2/2	LCOS	80	16	4	45	4.4	14	2	3	HIV3 K2 G2
A2	6–15	10 YR 2/2	LCOS	81	15	4	34	4.8	12	3	4	nr
A3	15–29	10 YR 3/3	LCOS	81	15	4	32	4.9	11	3	4	nr
A4	29–42	10 YR 3/3	LCOS	81	15	4	25	4.9	10	3	4	nr
Bw	42–63	10 YR 5/4	LCOS	84	13	3	11	5.2	6	2	5	K3 G3
BC	63–81	10 YR 6/6	LCOS	83	13	4	11	5.1	6	2	5	nr
R	81+		ROCK									

[a] C = COSL = coarse sandy loam, LCOS = loamy coarse sand, LS = loamy sand, ROCK = rock fabric, SCL = sandy clay loam, SL = sandy loam.
[b] G = Gibbsite, HIV = hydroxy-interlayered vermiculite, K = kaolin, M = mica; 1 = minor amount, 2 = moderate amount, 3 = major amount; nr = not reported.

(mid-elevation, below winter snowline) have hues as red as 2.5 YR, suggesting the additional component of hematite (Schwertmann, 1993). The Musick soils also have the highest clay contents (27%) and pedogenic iron (Fe_d) concentrations (14 g kg^{-1}), both of which occur in the strongly expressed argillic horizon. The other soils have much lower clay and Fe_d concentrations. The Musick soils, then, are the most intensely weathered and morphologically developed along the elevational transect. This is attributed to an optimal combination of temperature and moisture at this elevation, whereas weathering is inhibited at lower elevations by lack of moisture and at higher elevations by cold temperatures.

At the lowest elevation (Vista soils), the clay mineralogy consists of mica and kaolinite. The mica is mostly biotite inherited from the parent rock and the kaolinite is derived from plagioclase weathering. At somewhat higher elevations (data not shown), some of the mica has transformed to vermiculite and halloysite occurs with kaolinite. Halloysite has been shown to be the initial weathering product of plagioclase in forest soils with xeric moisture regimes in California (Southard and Southard, 1987; Takahashi et al., 1993). The halloysite subsequently dehydrates to exhibit x-ray diffraction behavior diagnostic of kaolinite.

In the mid-elevation soils (Musick series), kaolin minerals are the most abundant clay mineral group, with predominantly halloysite in the subsoil and kaolinite in the surface. This trend is consistent with the halloysite dehydration mechanism for the formation of kaolinite. Plagioclase sand grains are pseudomorphically replaced by tubular halloysite, as described in soils about 170 km to the north by Southard and Southard (1987). While mica is still a component of the clay fraction, some of it has weathered to vermiculite that has been hydroxy–Al interlayered in the more acid conditions at this elevation.

In the soils above the winter snowline (Shaver series and Cryepts), hydroxy-interlayered vermiculite becomes a dominant component of the clay fraction, along with kaolin and, in the Cryepts, gibbsite. The predominance of Al-rich and Si-depleted secondary minerals attests to the strong leaching regime that results from the melting of the winter snowpack each spring. Leaching intensity was interpreted to be the major factor determining the degree of desilication and mineral weathering along the transect.

3.3. Andesitic terrain of the northern Sierra Nevada

Northeastern California is dominated by volcanic terrain, comprising all of the Cascade Range and the Modoc Plateau, and large parts of the northern Sierra Nevada (Figs. 1 and 2). An elevational transect similar to the central Sierra Nevada transect on granitic terrain has been studied in the northern Sierra Nevada on volcanic materials (Rasmussen et al., 2007) and is discussed here to illustrate mineralogical trends in volcanic soils of northern California. Soils were investigated on pyroclastic mudflows of andesitic composition (lahars) at elevations ranging from 160 to 2700 m. The mean annual precipitation here is somewhat higher than in the central Sierra Nevada, ranging from 460 mm at the lowest elevation to 1520 mm at the highest elevation. Precipitation is dominantly snow at the sites above 1590 m and predominantly rain at the lower sites. The relationships between elevation and soil temperature and moisture regimes are similar to those in the central Sierra Nevada, as described above, as are the elevation — vegetation relationships. All of the soils in the transect were sampled on summit positions with 10 to 15% slopes to the west or southwest.

Four of the seven soils in the elevational transect will be highlighted here. At the lowest elevation (160 m), Xerolls (loamy-skeletal, mixed, superactive, thermic Ultic Haploxerolls) support oak woodlands dominated by blue oak (*Quercus douglasii*). At an intermediate elevation (1150 m) below the winter snowline, Humults (fine, parasequic, mesic Andic Palehumults) have a mixed conifer forest dominated by ponderosa pine (*Pinus ponderosa*). At a mid-elevation (1700 m) just above the winter snowline, the soils are Xerands with white fir (*Abies concolor*) dominating the conifer forest. In the subalpine forest at 2450 m elevation, Cryepts support red fir (*Abies magnifica*), Jeffrey pine (*Pinus jeffreyii*), and lodgepole pine (*Pinus contorta*).

The parent material mineralogy, as judged from very fine sand fractions and a rock sample, consisted of hornblende, plagioclase (andesine and albite), a chlorite-like mineral, cristobalite, tridymite, and quartz. Volcanic glass is present in relatively small amounts (<5%) in the soils at elevations <1500 m. In the higher elevation soils, volcanic glass makes up 10 to 30% of the very fine sand fraction. Volcanic activity in the Cascade Range and the eastern Sierra Nevada has persisted through the Holocene and may account for the occurrence of glass in these soils.

Selected soil properties are presented in Table 3. The low elevation soils (Xerolls) are underlain by hard bedrock (R horizon) at a shallow depth, have 10 YR and 7.5 YR hues, and clay contents of between 15 and 20%. Soils above the winter snowline (Xerands and Cryepts) are moderately deep over weathered bedrock and also have 10 YR and 7.5 YR hues but clay contents are generally 5 to 15%. The mid-elevation soils below the winter snowline (Humults) are very deep and red (5 YR hues) with a clayey argillic horizon (43% clay) extending below 200 cm. Dithionite-extractable Fe is also highest in these reddest soils. Here, as in the elevational transect on granitic rock, the mid-elevational soils immediately below the winter snowline are found to be the most intensely weathered and morphologically developed. The soils in this transect on andesite are generally redder and contain more clay and pedogenic iron oxides than soils at comparable elevations in granitic terrain to the south. It should be noted that, in addition to mafic mineral weathering, wildfires contribute to soil reddening through the thermal transformation of goethite to hematite or maghemite in places where large fuel items (e.g., logs) are thoroughly combusted on the soil surface (Ulery and Graham, 1993; Goforth et al., 2005).

The clay mineralogy of the low elevation soils (Xerolls) is dominated by kaolinite, with a trace of vermiculite. The mid-elevation soils below the winter snowline (Humults) are also dominated by kaolin, occurring as halloysite in the subsoil and as kaolinite or dehydrated halloysite near the surface. The kaolin at both sites is derived from the weathering of plagioclase, with halloysite as the initial weathering product, which is subsequently dehydrated under warmer, drier conditions (near surface or lower elevation). The Humults also contain gibbsite, derived from feldspar weathering, and hydroxy-interlayered vermiculite. This mineral assemblage, reflective of intense desilication, is consistent with soil morphologic indications of intensive weathering at this elevation. Only soils above the winter snowline (Xerands) contain an appreciable amount of short range-ordered aluminosilicates (allophane and imogolite). The abundance of allophane and imogolite was identified by selective dissolution analysis (e.g., high Al_o levels in Table 3), lack of distinct XRD peaks from the clay fraction, and characteristic spheres (allophane) and tubes (imogolite) observed using transmission electron microscopy. These short range-order minerals constitute the bulk of the clay fraction, but are accompanied by traces of kaolin (halloysite) and hydroxy-interlayered vermiculite. The high elevation Cryepts have relatively low levels of short range-ordered minerals. The clay fraction of these soils is dominated by a hydroxy-interlayered smectite (HIS) with a lesser amount of kaolin. The HIS in this soil, and the HIV at the other sites, is likely derived from the chlorite-like mineral in the parent material. Pyroclastic materials often contain 2:1 layer minerals that are chloritized to some degree due to hydrothermal alteration (e.g., Glasmann, 1982; Pevear et al., 1982).

Table 3
Properties of soils in an elevational transect on andesite in the northern Sierra Nevada (Rasmussen et al., 2007).

Horizon	Depth (cm)	Dry color	Texture[a]	Sand (%)	Silt (%)	Clay (%)	O.C. (g kg^{-1})	pH (1:1)	CEC$_7$ (cmol kg^{-1})	Fe$_d$ (g kg^{-1})	Al$_o$ (g kg^{-1})	Clay mineralogy[b]
160 m elevation: loamy-skeletal, mixed, superactive, thermic Lithic Ultic Haploxeroll												
A1	0–5	10 YR 5/4	L	43	40	17	36	6.2	30	16	2	nr
A2	5–14	7.5 YR 5/4	L	43	39	18	20	6.2	24	16	2	nr
Bw1	14–25	7.5 YR 5/4	L	47	34	19	12	6.2	22	17	2	K3 Vt
Bw2	25–42	7.5 YR 5/4	L	47	34	19	7	6.4	22	16	2	nr
R	42+		ROCK									
1150 m elevation: fine, parasequic, mesic, Andic Palehumult												
A	0–10	7.5 YR 3/3	L	38	38	24	89	6.2	44	37	15	nr
ABt	10–40	5 YR 4/4	CL	34	35	31	27	6.4	22	44	17	nr
Bt1	40–60	5 YR 4/6	CL	42	23	35	17	6.3	20	48	15	K2 HIV1 G1
Bt2	60–100	5 YR 4/6	C	35	25	40	5	6.1	17	53	6	nr
Bt3	100–158	5 YR 5/6	C	33	24	43	3	5.9	16	49	5	nr
Bt4	158–200	5 YR 5/6	C	35	22	43	2	5.8	15	47	4	nr
1700 m: medial-skeletal, amorphic, mesic Humic Haploxerand												
A1	0–19	7.5 YR 4/3	SL	62	34	4	120	6.3	40	13	31	nr
A2	19–32	7.5 YR 5/4	SL	58	36	6	69	6.2	27	15	37	nr
Bw1	32–48	7.5 YR 5/4	SL	66	28	6	46	6.0	23	16	39	SROM3 Kt HIVt
Bw2	48–83	7.5 YR 5/4	SL	69	25	6	31	5.9	18	14	34	nr
Cr	83+		ROCK									
2450 m elevation: loamy-skeletal, mixed, superactive Vitrandic Dystrocryept												
A1	0–7	10 YR 4/2	SL	69	20	11	62	5.8	30	10	6	nr
A2	7–19	10 YR 5/3	SL	66	22	12	21	5.8	20	10	7	HIS2 K1
AC1	19–37	10 YR 5/3	SL	69	18	13	12	6.0	19	10	7	nr
AC2	37–62	10 YR 5/3	SL	58	28	14	10	6.0	21	10	6	nr
Cr	62+		ROCK									

[a] C = clay, CL = clay loam, L = loam, ROCK = rock fabric, SL = sandy loam.
[b] G = gibbsite, HIS = hydroxy-interlayered smectite, HIV = hydroxy-interlayered vermiculite, K = kaolin, SROM = short range-ordered minerals, V = vermiculite; t = trace, 1 = minor amount, 2 = moderate amount, 3 = major amount; nr = not reported.

Even though consistency of soil age, and to some extent parent material uniformity (i.e., variation in volcanic ash deposition), cannot be fully assured, this elevational sequence shows the marked impact of climate on pedogenic mineral formation. The warmest, most moist soils in the mid-elevations are the most intensively weathered. The mid-elevation soils above the winter snowline, which also have a substantial amount of volcanic glass, were the only soils dominated by allophanic materials.

3.4. Fluvial terraces on the east side of the Great Valley

Throughout the Quaternary, materials eroded from the Sierra Nevada have been transported westward and deposited as alluvium in the Great Valley. Uplift and base level lowering have preserved portions of these alluvial deposits and their geomorphic surfaces as a series of terraces or alluvial fan remnants. The oldest surfaces are at the highest elevations and the youngest ones are closest to the current alluvial floodplains. A particularly well-preserved sequence of such terraces is found along the Merced and Tuolumne Rivers (Fig. 1) (Marchand and Allwardt, 1981; Harden, 1982). The deposits are primarily glaciofluvial sediments from the granitic terrain of the Sierra Nevada with minor amounts of metavolcanic and other more mafic rocks from the foothills. The soils on these preserved geomorphic surfaces form a chronosequence spanning a time period of three million years. Elevations are less than 200 m and the mean annual precipitation is about 300 mm. This precipitation occurs as rain

a

b

Fig. 8. Fluvial terrace landscapes in the Great Valley (Fig. 1); (a) mid-Pleistocene surface in the foreground and higher early Pleistocene surfaces on the horizon; (b) view across the early Pleistocene surface showing mima mounds. Note the swale (vernal pool) in the foreground collects water in the rainy season (photo credits: R. Amundson).

between October and May. The soils have a xeric moisture regime and a thermic temperature regime. The native ecosystems are grasslands with scattered oaks on the Holocene and late Pleistocene surfaces (Arkley, 1962). Most of the younger surfaces are valuable for cultivated crops, vineyards, and orchards. The older landscapes are grasslands used for cattle grazing (Fig. 8a). Slope gradients are nearly level (0–5%).

Three of the soils from the chronosequence are discussed here to illustrate soil mineralogical trends on landscape positions of different ages in the Great Valley. The soil on a 40 ka geomorphic surface is a coarse-loamy, mixed, active, thermic Typic Haploxeralf, the one on a 600 ka surface is a fine-loamy, mixed, semiactive, thermic Mollic Haploxeralf, and the soil on a 3000 ka surface is a fine, kaolinitic, semiactive, thermic Ultic Palexeralf. All indications of soil morphological development increase with age, including clay concentrations, subsoil redness, and dithionite-extractable iron (Table 4). Both Haploxeralfs have pH values near neutral, but the pH of the Palexeralf ranges between 4.0 and 4.9 (Harden, 1987, 1988). Some soils on the 3000 ka surface have silica-cemented duripans (Marchand and Allwardt, 1981).

The parent materials of the soils are arkosic sands and gravels derived from the granitic terrain of the central Sierra Nevada. As such, they are dominated by quartz, sodium-rich plagioclase (~$An_{0.32}$), and K-feldspar, with lesser amounts of hornblende (5–10%), biotite (~5%), and other heavy minerals (Marchand and Allwardt, 1981; Harden, 1987; White et al., 1996). The influence of the parent material on the soil clay mineralogy is apparent throughout the chronosequence. Mica (biotite) and its weathering products (vermiculite, interstratified mica/vermiculite) are major components in the coarse-loamy Haploxeralfs (40 ka), but decrease in relative abundance in the older soils (Table 4). Kaolinite, a weathering product of feldspars, increases in relative abundance with soil age, becoming particularly abundant in the Palexeralf. Smectite is not present in the coarse-loamy Haploxeralf and is a minor component in the fine-loamy Haploxeralf, but in the lower part of the Palexeralf it is very abundant. All of the clay fractions contain very small amounts of quartz and feldspar.

Hornblende and biotite are the only significant sources of Fe and are the most readily weathered components of the parent material (White et al., 1996). The iron oxides produced by the weathering of these minerals are responsible for the soil colors. The 10 YR hues of the Haploxeralfs indicate goethite, which likely predominates throughout the chronosequence even as hematite becomes the main pigmenting agent and produces redder hues in the fine-loamy Haploxeralf and the Palexeralf. Plagioclase weathers more quickly to kaolinite than does K-feldspar, but in the oldest soils (Palexeralfs) K-feldspar has contributed substantially to kaolinite production (White et al., 1996). Plagioclase is essentially depleted in the fine-loamy Haploxeralfs (600 ka), while significant K-feldspar persists in the 3,000 ka Palexeralfs.

Morphologic development, specifically the formation of clay-rich argillic horizons and duripans, changes the hydrologic behavior of the soils as they age (White et al., 2005). Soil solutions in the younger soils become seasonally concentrated by high evapotransporational flux and are occasionally flushed during high precipitation events. In contrast, the clayey argillic horizons and duripans in the older soils isolate the deeper zones from major changes in water content, inhibiting both leaching and evaporative concentration. As a result, mineral weathering in the deeper horizons of the oldest soils is controlled more directly by thermodynamic solubility relationships. Because it is protected from leaching, this subsoil environment attains concentrations of silica and base cations that favor smectite formation.

Surface water hydrology is also affected by the clayey argillic horizons and duripans in the soils of the older terraces. These landscapes often have a distinctive microtopography consisting of mima mounds with intervening swales (Fig. 8b). Due to the low-permeability of the argillic horizons and duripans, the swales collect water during the rainy season and are known as vernal pools (Rains et al., 2006; O'Geen et al., 2008). Soils in the swales are smectite-rich Alfisols and Vertisols.

Pore waters in the Haploxeralfs are generally undersaturated with respect to opal-A, except for periods of time, usually in the summer, when solute Si reaches opal-A saturation within and immediately below the argillic horizons. During the winter months, silica cementation appears to dissipate, apparently because the soil solution is then undersaturated with respect to opal-A and it dissolves. Some amorphous silica persists through the seasonal precipitation/dissolution

Table 4
Properties of soils on fluvial terraces in the Great Valley (Harden, 1987).

Horizon	Depth (cm)	Dry color	Texture[a]	Sand (%)	Silt (%)	Clay (%)	O.C. (g kg^{-1})	pH (1:1)	CEC_7 (cmol kg^{-1})	Fe_d (g kg^{-1})	Clay mineralogy[b]
40 ka terrace: coarse-loamy, mixed, active, thermic Typic Haploxeralf											
A1	0–15	10 YR 5/3	LFS	nr	nr	nr	nr	nr	nr	nr	nr
A2	15–81	10 YR 6/3	LS	80	14	6	2	6.5	3	3	M4 K3 Q2 F1
2Bt1	81–102	10 YR 5/4	LS	87	2	11	2	6.9	4	4	nr
3Bt2	102–170	10 YR 5/6	SL	79	4	17	1	6.7	8	5	K3 V3 M2 HIV1 M/V1 Q1 F1
4BC	170–201	10 YR 6/6	LS	86	8	6	4	7.0	6	4	nr
5C	201–231	10 YR 6/4	S	91	6	3	4	7.3	4	4	V3 K2 M/V1 M1 Q1 F1
600 ka terrace: fine-loamy, mixed, semiactive, thermic Mollic Haploxeralf											
Ap1	0–5	10 YR 5/2	LS	79	14	5	nr	6.8	11	4	nr
Ap2	5–11	10 YR 5/3	SL	74	16	7	6	7.0	4	6	K3 V2 M2 C1 CM1 Sm1 Q1 F1
AB	11–20	7.5 YR 5/4	SCL	63	15	21	nr	6.9	7	11	nr
Bt1	20–33	5 YR 4/6	SCL	58	12	29	nr	6.7	10	11	nr
Bt2	33–80	5 YR 5/6	SCL	64	9	26	nr	6.6	10	9	K4 V2 M2 CM1 Q1 F1
BCt1	80–191	5 YR 5/6	SCL	76	3	20	nr	6.9	9	8	nr
BCt2	191–256	5 YR 6/6	SL	79	3	18	nr	7.1	7	9	nr
BC	256–292	5 YR 6/6	SL	85	1	14	nr	7.0	7	5	nr
CB	292–375	7.5 YR 6/6	SL	84	1	14	nr	7.0	7	5	nr
3000 ka terrace: fine, kaolinitic, semiactive, thermic Ultic Palexeralf											
A	0–12	7.5 YR 6/6	L	37	46	17	3	4.8	7	14	K4 Q2 V1 M1 Sm1 F1
AB	12–53	7.5 YR 6/6	L	34	43	23	3	4.9	7	16	nr
2Bt1	53–88	5 YR 4/8	C	25	32	43	1	4.6	12	24	nr
2Bt2	88–140	5 YR 4/8	C	25	20	55	3	4.4	12	33	K4 Sm2 V1 M1 Q1 F1
2BCt1	140–234	2.5 YR 4/8	C	31	26	43	2	4.0	12	33	nr
2BCt2	234–310	2.5 YR 4/8	C	24	21	55	2	4.0	16	21	K4 Sm4 Q1 F1

[a]C = clay, L = loam, LFS = loamy fine sand, LS = loamy sand, S = sand, SCL = sandy clay loam, SL = sandy loam.
[b]C = chlorite, CM = chloritized mica, F = feldspar, HIV = hydroxy-interlayered vermiculite, K = kaolin, M = mica, M/V = interstratified mica/vermiculite, Q = quartz, Sm = smectite, V = vermiculite; 1 = minor amount, 2 = moderate amount, 3 = major amount, 4 = dominant; nr = not reported.

cycles, leading to the less soluble opal-CT that cements duripans in some of the 3,000 ka soils (White et al., 2005). Amorphous silica has been shown to progressively accumulate with age in similar soils in southern California (Kendrick and Graham, 2004).

3.5. Marine terraces of the central coast

Along much of coastal California, previous shorelines are marked by marine terraces (e.g., Merritts et al., 1991; Moody and Graham, 1995; Muhs et al., 2007). These terraces are wave-cut platforms that have been raised above sea level either by a lowering of sea level or tectonic uplift of the land. The platforms are cut into bedrock and subsequently covered by various beach and near-shore sediments and eolian deposits. Soils that develop on these marine terraces have been the subject of chronosequence studies because each terrace in a suite of marine terraces marks a discrete period of time at which soil formation began, the highest terraces being the oldest. The coastal climate of California has remained nearly constant since the late Pleistocene, with only somewhat cooler, wetter conditions during glacial periods (Johnson, 1977). Thus, climate change has not been a significant confounding factor in these chronosequences.

A well-characterized marine terrace chronosequence is found on the central coast at Santa Cruz (Figs. 1 and 9). The mean annual precipitation ranges from about 800 to 880 mm, increasing with elevation. The soils have a xeric moisture regime and a mesic moisture regime. The terrace surfaces slope slightly (<5%) toward the sea and have grassland vegetation. Soils from three of the terraces are discussed here. At an elevation of 14 m, soils are coarse-loamy, mixed, active, mesic Typic Argixerolls and are about 65 ka. The marine terrace at 116 m is about 137 ka and its soils are fine-loamy, mixed, semiactive, mesic Ultic Argixerolls. The oldest terrace (about 226 ka) is at 159 m and has fine, mixed, semiactive, mesic Typic Haploxerults (Pinney et al., 2002; Aniku and Singer, 1990; White et al., 2008). The sediments from which the soils are derived contain primarily quartz, plagioclase (An_{25}–An_{33}), and K-feldspars (White et al., 2008). There are lesser amounts of biotite and hornblende.

Several soil properties presented in Table 5 show progressive changes expected in such a chronosequence. The maximum redness increases from 10 YR hues in the Typic Argixerolls to 5 YR in the Ultic Argixerolls and 10 R in the Haploxerults. Maximum clay contents increase from 17 to 48 to 56% in the same sequence. Minimum soil pH values change from near neutral in the youngest soil to 4.8 in the oldest. Dithionite-extractable Fe concentrations increase from <10 g kg^{-1} in the youngest soil to >40 g kg^{-1} in the oldest.

Clay fraction components are relatively consistent throughout the chronosequence (Pinney et al., 2002). Kaolinite is the predominant phyllosilicate, followed by interstratified chlorite/vermiculite. Mica and gibbsite are minor components. Quartz and minor amounts of feldspar and Fe-rich dioctahedral smectite are inherited from the parent material (White et al., 2008). While the major clay fraction components are relatively constant, certainly their total amounts, as reflected by the increase in clay content, change considerably. Kaolinite production is the result of the weathering of smectite and feldspars (White et al., 2008), such that the oldest soils are appreciably depleted of smectite and the calcic phases of plagioclase. Presumably, the chlorite/vermiculite is a weathering product of chlorite in the initial deposits.

In contrast, kaolinite is a minor component in the soils of a marine terrace chronosequence on San Clemente Island, 550 km to the southeast of Santa Cruz. In those soils, mica and smectite are the dominant clay minerals (Muhs, 1982). The soils are formed in eolian material, which includes mica, that is blown from the Mojave Desert and southwestern California (Muhs et al., 2007). As the soils weather, the mica is transformed to smectite.

The prominent colors of the subsoils in the Santa Cruz chronosequence are due to Fe oxides that form coatings on the silicate grains. So even though the Fe oxides are present in relatively small amounts (<5%), their presence is highly visible. The change in soil redness with age suggests changes in Fe oxide mineralogy. As the 10 YR hues indicate, goethite is the only Fe oxide mineral in the Typic Argixerolls (65 ka). A small amount of hematite is present in the older soils, but, since hematite is such a strong pigmenting agent (Schwertmann, 1993), it is sufficient to redden the soils even though goethite is still

Fig. 9. Oblique aerial view of the Santa Cruz marine terraces (Fig. 1) (photo credit: copyright (C) 2002–2009 Kenneth & Gabrielle Adelman, California Coastal Records Project, <http://www.Californiacoastline.org>www.Californiacoastline.org).

Table 5
Properties of soils on marine terraces of the central coast (Pinney et al., 2002).

Horizon	Depth (cm)	Dry color	Texture[a]	Sand (%)	Silt (%)	Clay (%)	O.C. (g kg^{-1})	pH (1:1)	$CEC_{8.2}$ (cmol kg^{-1})	Fe_d (g kg^{-1})	Clay mineralogy[b]
65 ka terrace: coarse-loamy, mixed, active, mesic Typic Argixeroll											
A	0–29	10 YR 4/2	SL	69	22	9	11	6.8	5	5	nr
E	29–50	10 YR 5/2	SL	70	20	10	3	7.2	5	4	K3 C/V2 Q2 M1 G1 Sm1 F1
BE	50–90	10 YR 6/3	SL	68	17	15	1	7.3	7	5	nr
Bt1	90–106	10 YR6/3, 7.5 YR 6/6	SL	67	16	17	2	7.4	10	5	K3 C/V2 Q2 M1 G1 Sm1 F1
Bt2	106–170	2.5 Y 6/4	LS	84	3	13	<1	7.4	13	7	nr
C1	170–200	5 Y 7/2	S	96	2	2	<1	7.3	5	6	K1 M1 C/V1 G1 Sm1 Q1 F1
137 ka terrace: fine-loamy, mixed, semiactive, mesic Ultic Argixeroll											
A1	0–2.5	10 YR 4/3	SL	58	25	17	41	6.1	17	10	nr
A2	2.5–25	7.5–10 YR 4/3	SCL	53	25	22	16	6.4	13	14	K3 C/V2 Q2 M1 G1 F1
BA	25–60	7.5 YR 5/4	SCL	49	22	29	8	6.5	11	20	nr
Bt1	60–85	7.5 YR 5/6	SC	48	13	39	5	6.5	12	23	nr
Bt2	85–111	5 YR 4/3, 5/8	C	41	11	48	4	6.6	15	28	K3 C/V2 Q2 M1 G1 Sm1 F1
Bt3	111–158	7.5 YR 6/6	SCL	53	15	32	3	5.4	10	24	nr
BC1	158–220	7.5 YR 5/8, 10 YR 6/1	SCL	57	13	30	3	5.3	8	21	K3 C/V2 Q2 M1 G1 Sm1 F1
226 ka terrace: fine, mixed, semiactive, mesic Typic Haploxerult											
A1	0–2	10 YR 5/4	nr	nr	nr	nr	23	5.5	18	13	nr
A2	2–16	10 YR 5/3	SCL	52	27	21	15	5.3	12	18	K3 C/V2 Q2 M1 G1 Sm1 F1
E	16–24	10 YR 6/4	SCL	48	27	25	14	5.1	12	21	nr
Bt1	24–43	10 YR4.5/4	SCL	46	27	27	6	5.1	11	22	nr
2Bt2	43–74	10 YR 4/4, 10 R 4/6	C	38	13	49	3	5.1	15	37	K3 C/V2 Q2 M1 G1 F1
2Bt3	74–96	10 YR 4/4, 10 R 4/8, 2.5 YR 5/6	C	38	6	56	5	4.9	16	43	K3 C/V2 Q2 M1 G1 Sm1 F1
3BC1	96–185	7.5 YR 6/6, 2.5 YR 3/6	SCL	60	14	26	3	4.8	11	17	nr

[a]C = clay, LS = loamy sand, SC = sandy clay, SCL = sandy clay loam, SL = sandy loam.
[b]C/V = interstratified chlorite/vermiculite, F = feldspar, G = gibbsite, K = kaolin, M = mica, Q = quartz, Sm = smectite; 1 = minor amount, 2 = moderate amount, 3 = major amount; nr = not reported.

the predominant Fe oxide (Aniku and Singer, 1990). Another Fe oxide phase that increases with age in these soils is maghemite. This pedogenic ferromagnetic mineral is largely concentrated in nodules associated with the argillic horizons of the two older soils (Fine et al., 1992; Singer et al., 1995). These nodules contain up to half of the total Fe in those horizons (White et al., 2008). Maghemite has a reddish brown color (2.5 YR–5 YR hues) (Schwertmann, 1993), so in a finely divided form it would contribute to soil reddening. Maghemite is formed by heating goethite under slightly reducing conditions, as under large fuels in wildfires, or by oxidation of magnetite (Bigham et al., 2002). The latter is the more likely origin in the Santa Cruz soils, where magnetite is present in all of the soils, but is depleted by weathering at shallower depths and with increasing age (Fine et al., 1992).

In marine terraces 210 km to the southeast, opaline silica is an important soil component. Along with Fe oxides and clay, opal-A plugs the matrix pores in the deeper regolith (20–50 m) so that water flow is diverted to fractures and channels, which then become depleted of Fe oxides (Moody and Graham, 1994). Opaline silica also concentrates at and near the scarps of terrace edges (Moody and Graham, 1997). Water flows laterally through soils toward drainages that dissect the terrace surface. Evaporation from the terrace scarps concentrates the soil solution such that it is supersaturated with respect to opaline silica. Silica precipitates at the scarp surface and several meters back into the soil, cementing the soil material in such a way that blockfall is the predominant form of erosion along the terrace edges. Sources of silica in these materials include the weathering of feldspars and chert.

3.6. Ultramafic terrain of the Klamath Mountains

The largest area of ultramafic terrain in North America is in the Klamath Mountains, a steep, rugged region with relatively high rainfall (Lee et al., 2004). The ultramafic rocks there consist of peridotites and serpentinites in several ophiolite belts that roughly parallel the continental margin. The minerals that make up the rocks contain abundant Mg and Fe, but very low levels of Ca and Al, and virtually no K. Soils derived from these ultramafic rocks are of interest because they represent a geochemical extreme that has a dramatic impact on secondary mineral formation and on ecosystem composition and productivity. While much of the Klamath Mountains is underlain by non-ultramafic lithology, such as granitic and metasedimentary rocks, and is densely forested, the ultramafic areas typically have sparse and relatively stunted trees. This characteristic of low biomass and low productivity, together with the occurrence of endemic species, is referred to as the "serpentine syndrome" (Alexander et al., 2007). Landslides are common in the Klamath serpentinite areas because of the steep slopes, high rainfall, and structural instability imparted by serpentine and smectite. Smectite, a common weathering product of serpentine minerals, expands when wet, thereby reducing the shear strength of the materials in which it is found. Large, stabilized rotational slumps are common landscape features in this region.

The relationships of soil mineralogy and geomorphic position were studied in an area of serpentinized peridotite encompassing a stabilized landslide bench and surrounding slopes (Figs. 1 and 10) (Lee et al., 2003, 2004). The study site is within the Trinity ophiolite complex, the largest ultramafic body in the Klamath Mountains. The elevation of the site is about 1200 m and the mean annual precipitation is 1000 mm, falling as rain and snow almost entirely between October and May. Several small springs and ephemeral creeks from the headwall scarp deliver water to the landslide bench where it is ponded behind the landslide bulge to form a seasonally wet meadow. The vegetation in the meadow consists of grasses, sedges, rushes, and forbs. The surrounding slopes support open stands of Jeffrey pine (*Pinus jeffreyii*) and incense cedar (*Calocedrus decurrens*) with a scattered understory of buckbrush (*Ceanothus cuneatus*) and California fescue (*Festuca californica*). Slopes range from >30% on the scarp to ≤10% on the landside bench.

Two soils from a toposequence across the ultramafic landslide terrain are used here as an example to illustrate weathering and secondary mineral formation (Table 6). The soils on the backslope of a ridge flanking the wet meadow are Argixerolls (clayey-skeletal, magnesic, mesic Aquic Argixerolls). Soils on the toeslope within the wet meadow itself are Endoaquolls (fine, magnesic, mesic Cumulic Endoaquolls).

Fig. 10. Ultramafic terrain in the Klamath Mountains (Fig. 1) showing open Jeffrey pine — incense cedar forest on slopes surrounding a wet meadow (photo credit: B. Lee).

The Argixerolls are formed in 100-cm-thick colluvium which overlies >60 cm of soft, weathered bedrock (Cr1 and Cr2 horizons). The brown colors are suggestive of goethite, the common Fe oxide produced from serpentinite weathering. Clay content increases from about 30% in the A horizon to a maximum of 40% in the Bt3 horizon, then drops sharply to 6% in the Cr horizon. The pH increases with depth, from 6.3 in the A horizon to 7.8 in the Cr2. The Endoaquolls have formed in deep landslide colluvium. Low chroma colors are produced by predominating reducing conditions and relatively high organic matter contents (35–121 g kg^{-1} organic C). Clay content is high (45–58%) throughout and pH is between 6 and 7. Dithionite-extractable Fe is higher in the more oxidizing environment of the upslope Argixerolls than in the Endoaquolls. In both soils, Mn oxide content (Mn_d) increases upward in the soil, reflecting the more oxidizing environment near the surface.

Within the Klamath Mountains, and ultramafic terrain elsewhere in the state, a mix of yellow-brown and reddish colors can be observed in the landscape. The cause of this color variation is related to the mineralogical source of Fe (Alexander, 2004). While serpentinite and peridotite may contain roughly the same amount of Fe, the Fe in peridotite is contained within easily weathered minerals, such as olivine, whereas in serpentinite Fe is mostly in magnetite, which is very resistant to weathering. Thus, in peridotite-derived soils the Fe is released rapidly and abundantly, favoring the formation of hematite (Bigham et al., 2002) which imparts red coloration. In serpentinite-derived soils, the recalcitrant magnetite is minimally weathered and only low levels of Fe are released from serpentine weathering, a situation that favors goethite formation and corresponding yellow-brown colors.

Table 6
Properties of soils in a toposequence on serpentinized peridotite in the Klamath Mountains (Lee et al., 2003).

Horizon	Depth (cm)	Dry color	Texture[a]	Sand (%)	Silt (%)	Clay (%)	O.C. (g kg^{-1})	pH (1:1)	$CEC_{7.0}$ (cmol kg^{-1})	Fe_d (g kg^{-1})	Mn_d (g kg^{-1})	Clay mineralogy[b]
Backslope/forest: clayey-skeletal, magnesic, mesic Aquic Argixeroll												
O	2–0											
A	0–6	1 Y 4/2	CL	35	36	29	65	6.3	42	21	0.9	Sp3 C3 Sm_L3 T2 A1
Bt1	6–24	1 Y 4/2	CL	35	33	32	46	6.2	39	21	0.8	nr
Bt2	24–43	1 Y 5/2	CL	32	31	37	24	6.4	39	24	0.6	Sm_L4 C2 Sp3 T1 A1
Bt3	43–69	2 Y 5/3	CL	31	29	40	12	6.7	48	22	0.4	nr
BC	69–100	5 Y 5/3	SCL	50	26	24	3	7.2	56	14	0.3	$Sm_{H,L}$4 T1 Sp1 C1
Cr1	100–134	3 Y 5/2	ROCK	64	30	6	2	7.7	50	2	0.1	nr
Cr2	134–161	8 Y 6/2	ROCK	61	32	7	2	7.8	46	2	<0.1	$Sm_{H,L}$ V C C/V
Toeslope/meadow: fine, magnesic, mesic Cumulic Endoaquoll												
A	0–4	10 YR 4/1	C	nr[c]	nr	nr	121	6.6	53	11	0.7	nr
Bw	4–16	2 Y 4/1	C	30	25	45	46	6.7	51	13	0.8	Sm_L4 Sp3 T2 C2
Bg1	16–38	2 Y 4/1	C	22	20	58	42	6.7	60	13	0.6	nr
Bg2	38–100	2 Y 4/1	C	27	24	49	35	6.8	56	13	0.4	Sm_L4 Sp3 T2 C1
Bg3	100–156	2 Y 4/1	C	17	25	58	40	6.9	58	17	0.5	Sm_L4 Sp3 T2 C1
Bg4	156–200	2 Y 4/1	C	15	28	57	54	6.1	62	12	0.2	nr

[a] C = clay, CL = clay loam, ROCK = rock fabric, SCL = sandy clay loam.
[b] A = amphibole, C = chlorite, C/V = interstratified chlorite/ vermiculite, Sm_L = low-charge smectite, Sm_H = high-charge smectite, Sp = serpentine, T = talc, V = vermiculite; 1 = minor amount, 2 = moderate amount, 3 = major amount, 4 = dominant; nr = not reported.
[c] nr = not reported.

In the study by Lee et al. (2003), serpentine and Fe-rich chlorite are the two main primary minerals in the parent material, but talc, amphibole, and quartz are minor and variable components as well. Chlorite, serpentine, talc, and amphibole persist into the clay fraction in these soils. Smectite is the dominant secondary mineral, but it is not a single phase. A high-charge smectite forms through the transformation of chlorite. The chlorite weathers via loss of the interlayer hydroxide sheet, yielding both regularly and randomly interstratified chlorite/vermiculite and, with complete loss of the interlayer sheet, vermiculite. The chlorite-derived vermiculite further alters to high-charge smectite in the lower horizons of the Argixeroll. On the other hand, most of the smectite in these soils is a low-charge, poorly ordered, Mg-rich, dioctahedral phase interpreted to have precipitated from the abundant Mg and silica released into solution by serpentine weathering. A stability diagram plotted with soil solution concentrations indicates that Mg-rich montmorillonite is stable in these soils.

The occurrence of clayey, smectite-rich soils in lower slope positions is typical of serpentinitic landscapes (Istok and Harward, 1982), because the main products of serpentine dissolution, Mg and silicic acid, are water soluble and are transported downslope where they concentrate to create conditions favorable for smectite precipitation. Other studies have found the smectite to be saponite (trioctahedral with Mg in the octahedral sheet) (Wildman et al., 1968; Senkayi, 1977), but at this site the neoformed smectite was dioctahedral. Apparently, there was sufficient Al in the system to allow formation of montmorillonite.

Some soils in ultramafic terrain support vegetation that is inconsistent with the "serpentine syndrome". Laboratory analyses show that these soils have atypically high exchangeable Ca:Mg ratios and contain Ca-rich primary minerals. Soils such as these have at least some contribution from a non-ultramafic source, such as colluvium (Lee et al., 2001) or lithologic inclusions McGahan et al., 2008).

3.7. Alluvial fan in the Mojave Desert

Alluvial fans are characteristic geomorphic features in the Mojave Desert, and in deserts around the world. A fan forms at the mouth of an intermittent stream channel where it emerges from a mountain canyon into a valley. The materials in an alluvial fan are a mix of the lithologies present in the watershed. Sediments in the alluvial fan are sorted by particle-size as a function of distance from the mountain front. The coarsest (heaviest) material is deposited first, at the apex of the fan, and the finer material is transported farther into the valley. Transport is by stream flow, debris flow, and mud flow processes.

Soils along a 7.5-km-long alluvial fan in the western Mojave Desert (Figs. 1 and 11) were studied by Strathouse (1982) and three of them are used here to illustrate soil mineralogical trends for the region (Table 7). The elevation of the fan ranges from 838 to 914 m. The area has cool winters and hot, dry summers. Mean annual precipitation is about 220 mm, most of which falls as rain in the winter, though scattered thunderstorms do occur in the summer. The soil moisture regime is aridic and the temperature regime is thermic. Vegetation includes creosote bush (*Larrea tridentata*), hop-sage (*Grayia spinosa*), burro-weed (*Ambrosia dumosa*), Joshua tree (*Yucca brevifolia*), and, on the lower parts of the fan, shadscale (*Attriplex canescens*). The alluvial fan contains a mix of lithologies including granite, quartzite, marble, and basalt.

Calcic Petrocalcids (sandy-skeletal, mixed, thermic, Calcic Petrocalcids) are found on the upper part of the fan (Table 7). These soils contain 25 to 37% rock fragments and mostly ≤5% clay. The pH is 8.7 to 8.9, reflective of sodium carbonate presence. Exchangeable Na percentage (ESP) is mostly 3 to 7 dS m^{-1} and salinity, as indicated by EC, is also low (≤1 dS m^{-1}). There is a petrocalcic horizon, with its upper surface at the 79 cm depth, in which clay content (14%) is somewhat higher than in the horizons above. This is also true for ESP (18%) and $CaCO_3$ (38%). Soils on the middle part of the fan are Xeralfic Petrocalcids (loamy, mixed, thermic, superactive, shallow Xeralfic Petrocalcids). They contain <1% rock fragments and have clay contents that range from 6% in the A horizons to a maximum of 16% in the argillic (Btk) horizon. The pH is ≥8.4 throughout, and is nearly one unit higher in the petrocalcic and underlying horizon, suggestive of Na carbonates. The ESP is ≤4 above the petrocalcic, but is 36 in the petrocalcic and 78 in the underlying horizon. The EC is ≤1 dS m^{-1}, except in the horizon below the petrocalcic, which has an EC of 5 dS m^{-1}. The $CaCO_3$ content of the petrocalcic horizon is 42%, whereas in the other horizons it is ≤15%. Natrargids (fine, smectitic, thermic Xeric Natrargids) are found on the lower, distal part of the fan. For the most part, they contain <10% rock fragments. Clay content increases from 4% in the uppermost horizon to a maximum of 50% in the natric (Btn) horizon. The pH ranges within values indicative of $CaCO_3$. The ESP is mostly within the range of 30 to 45, but is much lower in the surface horizons. The $CaCO_3$ content is relatively low except in the Btkn horizons (26–29%). The surface A horizons of the soils contain vesicular pores, a common feature of desert soils. These vesicular horizons reduce infiltration and leaching so that

Fig. 11. Alluvial fan landscape in the Mojave Desert (Fig. 1). Note desert pavement in the foreground (photo credit: A. Ohtomi).

Table 7
Properties of soils along an alluvial fan transect in the western Mojave Desert (Strathouse, 1982).

Horizon	Depth (cm)	Dry color	Texture[a]	Sand (%)	Silt (%)	Clay (%)	O.C. (g kg^{-1})	pH (1:1)	CEC$_{8.2}$ (cmol kg^{-1})	ESP	EC (dSm^{-1})	$CaCO_3$ (%)	Clay mineralogy[b]
Upper fan: sandy-skeletal, mixed, thermic Calcic Petrocalcid													
Avk	0–10	10 YR 6/4	COSL	73	22	5	1.3	8.7	6	3	<1	16	Q4 Sm3 K2 C1 M1
Bk1	10–51	10 YR 6/4	COS	91	6	3	0.3	8.9	3	7	<1	22	Q3 Sm3 K2 M1 P1 C1
Bk2	51–79	10 YR 6/4	COS	91	5	4	0.8	8.8	3	6	<1	21	Q3 Sm3 P2 K2 M2 C1
Bkkm	79–147	10 YR 8/1	COSL	64	22	14	0.8	8.9	6	18	1	38	P4 Q3 Sm2 K2 C1 M1
Middle fan: loamy, mixed, thermic, superactive, shallow Typic Petroargid													
Avk	0–13	10 YR 6/3	LS	77	17	6	1.0	8.4	7	nr[c]	<1	5	nr
Ak	13–30	10 YR 6/3	COLS	83	11	6	0.6	8.5	6	3	<1	3	Q4 K3 M2 C2
Btk	30–41	10 YR 6/4	SL	66	18	16	1.6	8.4	10	4	<1	15	Q4 Sm3 P3 K3 M2
Bkkm	41–81	10 YR 8/1	SL	54	32	14	1.3	9.3	4	36	1	42	P4 Q2 Sm1 C1 M1 K1
BCk	81–135	10 YR 6/4	COSL	75	15	10	0.2	9.2	5	78	5	10	P4 Q3 Sm2 K2 C1 M1
Lower fan: fine, smectitic, thermic Typic Natrargid													
Avk	0–25	10 YR 6/4	LS	82	14	4	0.8	8.6	6	3	<1	nr	nr
Ak	25–41	10 YR 6/4	SL	59	22	19	0.9	8.8	11	14	<1	<1	Q4 Sm2 M2 K2 C1
Bkn	41–51	10 YR 5/4	SCL	56	16	28	1.5	8.8	18	29	2	4	Q4 Sm3 M2 K2
Btkn	51–74	5 YR 5/6	C	44	8	48	1.5	8.2	37	33	7	2	nr
Btn	74–84	7.5 YR 5/6	C	42	8	50	1.0	7.9	38	39	14	<1	Q4 Sm3 M2 K1
Btkn1	84–104	10 YR 7/3	CL	37	26	37	1.1	8.0	21	44	13	26	Sm3 Q3 P2 M2 K2
Btkn2	104–119	10 YR 6/6	CL	42	30	28	1.2	7.9	20	44	13	29	Sm3 Q3 P1 M1 K1
BCkn1	119–137	10 YR 6/4	COSL	63	21	16	0.3	8.1	20	38	14	2	nr
BCkn2	137–152	10 YR 6/6	SL	53	33	14	0.7	8.0	22	41	14	9	Sm4 Q2 M1 K1

[a] C = clay, CL = clay loam, COLS = coarse loamy sand, COSL = coarse sandy loam, COS = coarse sand, LS = loamy sand, SCL = sandy clay loam, SL = sandy loam.
[b] C = chlorite, K = kaolin, M = mica, P = palygorskite, Q = quartz, Sm = smectite; 1 = minor nt, 2 = moderate amount, 3 = major amount, 4 = dominant; nr = not reported.
[c] nr = not reported.

salts tend to accumulate in the underlying subsoils (Young et al., 2004; Wood et al., 2005; Graham et al., 2008). The dominant hue for soils along the transect is 10 YR, with only the Btkn and Btn horizons being appreciably redder. The high concentration of finely divided $CaCO_3$ in the petrocalcic horizons makes them white.

Dust deposition is a ubiquitous process in the Mojave Desert, delivering on the order of 2 to 20 g m^{-2} of sediment annually (Reheis, 2006). The dust originates from playas and active fluvial channels. The mineralogy of the dust varies with the source, but its clay fraction is consistently dominated by smectite and mica, with variable amounts of quartz, and lesser amounts of kaolinite and chlorite (Reheis and Kihl, 1995). This same suite of minerals occurs in the clay fraction of the soils on the alluvial fan highlighted here (Table 7). Some portion of these minerals has been inherited from the alluvium or, in the case of kaolin and smectite, derived by weathering in situ. Feldspars, biotite, and hornblende in rocks and sand grains extracted from the soils were partially altered to clay minerals. On the other hand, dust has certainly contributed significantly, at least on the upper fan where a desert pavement (Fig. 11) acts to trap dust (McFadden et al., 1987; Anderson et al., 2002). At a site 180 km to the east, soils developed on alluvial fans of various lithologies and ranging in age from 4 to 200 ka, had relatively uniform clay mineralogies and little evidence of primary mineral weathering (Deng and McDonald, 2007). The uniform clay mineralogy across age and lithology was interpreted to indicate that weathering of the alluvium contributed relatively little to soil clay mineralogy compared to eolian dust inputs, which with time are translocated into subsoils.

In the study by Strathouse (1982) highlighted here, x-ray diffraction patterns of the clay fraction of some of the horizons contained a 1.08-nm peak, which was especially intense in the petrocalcic horizons. This peak was originally identified as a partially altered mica, but is reinterpreted here as palygorskite (Table 7). Palygorskite was not widely recognized as a pedogenic mineral at the time of the study (Zelazny and Calhoun, 1977), but is now understood to commonly form in or immediately under petrocalcic horizons, including those in the Mojave and adjacent desert regions (McFadden, 1982; Graham and Franco-Vizcaíno, 1992; Reheis et al., 1992; Brock and Buck, 2007; Deng and McDonald, 2007). The high pH values and high Mg and Si activities in the localized petrocalcic environment are conducive to palygorskite neoformation (Singer, 2002).

All of the soils along the alluvial fan transect contain $CaCO_3$ in the form of calcite (Table 7). Calcite is present in most soils in the Mojave Desert and it becomes more abundant with soil age (Harden et al., 1991). Much of this calcite is deposited as dust (Reheis and Kihl, 1995), but it is also derived in situ from carbonate rock detritus (e.g., limestone, marble) if it is present. The dust is translocated into the soil (Anderson et al., 2002), where the calcite is dissolved and then

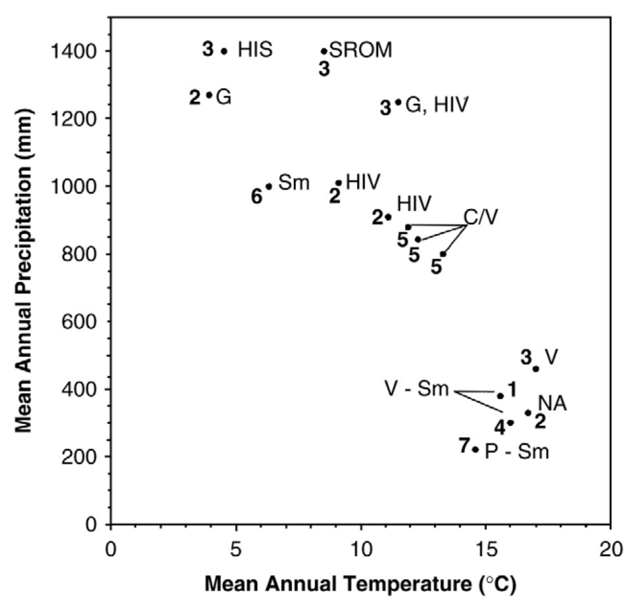

Fig. 12. The occurrence of major pedogenic clay minerals in California subsoils in relation to mean annual temperature and precipitation. Kaolin minerals are not included, but they occur (and often dominate) at all sites, except in ultramafic terrain. Study sites are indicated by numbers as in Fig. 1: (1) granitic terrain of the Peninsular Ranges, (2) granitic terrain of the central Sierra Nevada, (3) andesitic terrain of the northern Sierra Nevada, (4) fluvial terraces on the east side of the Great Valley, (5) marine terraces of the central coast, (6) ultramafic terrain of the Klamath Mountains, (7) alluvial fan in the Mojave Desert. Mineral abbreviations: C/V = interstratified chlorite/vermiculite, G = gibbsite, HIS = hydroxy-interlayered smectite, HIV = hydroxy-interlayered vermiculite, NA = not applicable (kaolin was the only pedogenic clay mineral), P = palygorskite, Sm = smectite, SROM = short range-ordered minerals, V = vermiculite. Hyphen between letters indicates local variation due to topography or age.

Table 8
Origin of soil clay minerals in representative California landscapes.[a]

	Peninsular R.	Sierra Nevada		Great Valley	Central Coast	Klamath Mts.	Mojave Desert
	Granitic	Granitic	Andesite	Fluvial terraces	Marine terraces	Serpentinite	Alluvial fan
Inherited							
Initial material	M	M	C	M, C	Sm, M, C	Sp, C, T	M, C
Eolian							Sm, K, C, M
Transformed	M → HB, V V → M	M → HIV	C → V, HIV, HIS	M → V, HIV	C → C/V	C → Sm_H C → V, C/V	M → Sm
Neoformed	K, Sm	K, G	K, G, SROM	K, Sm	K, G	Sm_L	P, Sm, K

[a]C = chlorite, C/V = interstratified chlorite/vermiculite, G = gibbsite, HB = hydrobiotite, HIS = hydroxy-interlayered smectite, HIV = hydroxy-interlayered vermiculite, K = kaolin, M = mica, P = palygorskite, Sm = smectite, Sm_H = high-charge smectite, Sm_L = low-charge smectite, Sp = serpentine, SROM = short range-ordered minerals, T = talc, V = vermiculite.

reprecipitated at a depth that reflects the depth of leaching (McFadden and Tinsley, 1985). Both the stable isotope composition and crystal morphology of pedogenic calcite vary with elevation on an alluvial fan and associated stream terraces 250 km northeast of the site addressed here (Amundson et al., 1989; Chadwick et al., 1989).

Opaline silica is a common component of carbonate-rich horizons in the Mojave (e.g., Boettinger and Southard, 1991; Eghbal and Southard, 1993), often to the point where it is the primary cementing agent. Such horizons are a kind of duripan (Soil Survey Staff, 1999) that cannot be visually distinguished from a petrocalcic horizon (cemented by $CaCO_3$).

The soluble salt content increases down the fan (Table 7) and gypsum (data not presented) was found only in the lowest part of the fan, in the Natrargid. Soluble salts and gypsum are also widely delivered to Mojave landscapes in dust (Reheis and Kihl, 1995), then dissolved and redistributed into soils with infiltrating water and to lower landscape positions with runoff water. The landscape distribution of soluble salts also depends on the direction of prevailing winds relative to the sources, which are playa surfaces (Hirmas, 2008). The depth distribution of salts, including chlorides, sulfates, and nitrates, depends on the degree of leaching that the soil experiences. Soils with minimal leaching, such as those mantled by desert pavement, have salts near the surface (Wood et al., 2005; Graham et al., 2008). Soils with high water tables, such as wet playas, have evaporite desposits on the surface and contribute salts to the eolian dust load (Reheis, 2006).

4. Synthesis and conclusions

The observation that kaolinite is the most ubiquitous phyllosilicate in soils (White and Dixon, 2002) is certainly relevant in California. Kaolin is present in all of the soils reviewed in this paper, irrespective of climate, parent material, age, or topographic position, except for those soils derived from ultramafic rocks. The investigations summarized here found ample evidence of kaolin forming via feldspar weathering, and that is probably the major source, but it can also form through weathering of other aluminosilicate minerals and by neoformation. It does not form in ultramafic soils because the parent materials contain insufficient Al.

The occurrence of secondary clay minerals other than kaolin reflects a climatic influence (Fig. 12). Palygorskite, smectite, and vermiculite occur in soils of dry, hot environments, whereas hydroxy-interlayered minerals, gibbsite, and short range-ordered minerals are in soils of cool, moist environments. Hot, humid and cold, dry environments are not well represented in California; nevertheless, the spectrum of clay minerals is displayed because broad relationships of soil clay mineralogy are often best correlated with mean annual precipitation, rather than temperature (Birkeland, 1999). The amount of precipitation is important because percolating water leaches silica from soils and differentiates the kinds of clays that can form.

The origins of minerals in soils can be placed into three general categories, (i) inheritance from parent materials, (ii) transformation from primary minerals, and (iii) neoformation (e.g., precipitation from solution) (Allen and Hajek, 1989). These three general sources contribute clay minerals to all of the pedogenic settings examined in this review (Table 8). Mica, particularly biotite, and chlorite are commonly inherited clay minerals. They are readily transformed to vermiculite, smectite, hydroxy-interlayered minerals, or interstratified minerals. Kaolinite, halloysite, gibbsite, short range-ordered minerals, smectite, and palygorskite are neoformed in various soil environments.

Iron oxides in California soils have been less studied, but several trends are apparent. Goethite is the most common and abundant pedogenic Fe oxide, imparting yellow brown colors. Those colors can be over-ridden by the strong red-pigmenting characteristic of hematite, which is evident in soils that are highly weathered due to age or a favorable weathering environment. The presence of easily weathered Fe-bearing minerals promotes the formation of hematite. Maghemite forms via oxidation of magnetite, but both it and hematite are also produced by thermal transformation of goethite during forest fires.

Calcite and opal-A occur in semi-arid and arid regions, whereas gypsum and the more soluble salts are found in the most arid landscapes. The landscape distribution of these minerals is often strongly related to patterns of eolian dust deposition and water infiltration and leaching.

Acknowledgements

The authors are grateful to Craig Rasmussen, Marjorie Schulz, and Jennifer Harden for providing additional information relative to their work on California soils. We also thank Judy Turk for preparing Fig. 1 and assisting with Fig. 12. Two anonymous reviewers provided comments that substantially improved the manuscript.

References

Agassi, M., Letey, J., Farmer, W.J., Clark, P., 1995. Soil erosion contribution to pesticide transport by furrow irrigation. Journal of Environmental Quality 24, 892–895.
Alexander, E.B., 2004. Serpentine soil redness, differences among peridotite and serpentinite materials, Klamath Mountains, California. International Geology Review 46, 754–764.
Alexander, E.B., Coleman, R.G., Keeler-Wolf, T., Harrison, S., 2007. Serpentine Geoecology of Western North America. Oxford Univ. Press, New York, NY.
Allen, B.L., Hajek, B.F., 1989. Mineral occurrence in soil environments. p. 199–278. In: J.B. Dixon and S.B. Weed (Editors), Minerals in Soil Environments. 2nd ed. Soil Science Society of America, Madison, WI.
Amundson, R.G., Chadwick, O.A., Sowers, J.M., Doner, H.E., 1989. The stable isotope chemistry of pedogenic carbonates at Kyle Canyon, Nevada. Soil Science Society of America Journal 53, 201–210.
Anderson, K., Wells, S., Graham, R., 2002. Pedogenesis of vesicular horizons, Cima volcanic field, Mojave Desert, California. Soil Science Society of America Journal 66, 878–887.
Anderson, M.A., Graham, R.C., Alyanakian, G.J., Martynn, D.Z., 1995. Late summer water status of soils and weathered bedrock in a giant sequoia grove. Soil Science 160, 415–422.
Aniku, J.R.F., Singer, M.J., 1990. Pedogenic iron oxide trends in a marine terrace chronosequence. Soil Science Society of America Journal 54, 147–152.
Arkley, R.J., 1962. Soil survey of Merced Area, California. U.S. Dep. Agric., Soil Conservation Service. In U.S. Gov. Print. Office, Washington, DC.
Baker, J.B., Southard, R.J., Mitchell, J.P., 2005. Agricultural dust production in standard and conservation tillage systems in the San Joaquin Valley. Journal of Environmental Quality 34, 1260–1269.
Bigham, J.H., Fitzpatrick, R.W., Schulze, D.G., 2002. Iron oxides. p.323–366. In: J.B. Dixon and D.G. Schulze (Editors), Soil Mineralogy with Environmental Applications. Soil Science Society of America, Madison, WI.
Birkeland, P.W., 1999. Soils and Geomorphology. Oxford Univ. Press, New York, NY.

Boettinger, J.L., Southard, R.J., 1991. Silica and carbonate sources for Aridisols on a granitic pediment, western Mojave Desert. Soil Science Society of America Journal 55, 1057–1067.
Brock, A., Buck, B.J., 2007. Pedogenic barite, palygorskite, and sepiolite in petrocalcic horizons at Mormon Mesa, Nevada: implications for soil water movement. GSA Abstracts with Programs, vol. 39, no. 6, p. 248.
Chadwick, O.A., Sowers, J.M., Amundson, R.G., 1989. Morphology of calcite crystals in clast coatings from four soils in the Mojave Desert region. Soil Science Society of America Journal 53, 211–219.
Clayton, J.L., Arnold, J.F., 1972. Practical grain size, fracturing density and weathering classification of intrusive rocks of the Idaho Batholith. USDA-FS Gen. Tech. Rep. INT-2. Intermountain For. Range Exp. Stn., Ogden, UT.
Dahlgren, R.A., Boettinger, J.L., Huntington, G.L., Amundson, R.G., 1997. Soil development along an elevational transect in the western Sierra Nevada, California. Geoderma 78, 207–2236.
Deng, Y., McDonald, E.V., 2007. Mineral occurrence, translocation, and weathering in soils developed on four types of carbonate and non-carbonate alluvial fan deposits in Mojave Desert, southeastern California. AGU Fall Meeting Abstract #B23B-1268.
Eghbal, M.K., Southard, R.J., 1993. Micromorphological evidence of polygenesis of three Aridisols, western Mojave Desert, California. Soil Science Society of America Journal 57, 1041–1050.
Fine, P., Singer, M.J., Verosub, K.L., 1992. Use of magnetic-susceptibility measurements in assessing soil uniformity in chronosequence studies. Soil Science Society of America Journal 56, 1195–1199.
Frazier, C.S., Graham, R.C., 2000. Pedogenic transformation of fractured granitic bedrock, southern California. Soil Science Society of America Journal 64, 2057–2069.
Frenkel, H., Goertzen, J.O., Rhoades, J.D., 1978. Effects of clay type and content, exchangeable sodium percentage, and electrolyte concentration on clay dispersion and soil hydraulic conductivity. Soil Science Society of America Journal 42, 32–39.
Glasmann, J.R., 1982. Alteration of andesite in wet, unstable soils of Oregon's Western Cascades. Clays and Clay Minerals 30, 253–263.
Goforth, B.R., Graham, R.C., Hubbert, K.R., Zanner, C.W., Minnich, R.A., 2005. Spatial distribution and properties of ash and thermally altered soils after high-severity forest fire, southern California. International Journal of Wildland Fire 14, 343–354.
Graham, R.C., Franco-Vizcaíno, E., 1992. Soils on igneous and metavolcanic rocks in the Sonoran Desert of Baja California, Mexico. Geoderma 54, 1–21.
Graham, R.C., Schoeneberger, P.J., Anderson, M.A., Sternberg, P.D., Tice, K.R., 1997. Morphology, porosity, and hydraulic conductivity of weathered granitic bedrock and overlying soils. Soil Science Society of America Journal 61, 516–522.
Graham, R.C., Hirmas, D.R., Wood, Y.A., Amrhein, C., 2008. Large near-surface nitrate pools in soils capped by desert pavement in the Mojave Desert, California. Geology 36, 259–262.
Harden, J.W., 1982. A quantitative index of soil development from field descriptions: examples from a chronosequence in central California. Geoderma 28, 1–28.
Harden, J.W., 1987. Soils developed in granitic alluvium near Merced, California. In: Harden, J.W. (Ed.), A Series of Soil Chronosequences in the Western United States: U.S. Geol. Surv. Bull., vol. 1590a.
Harden, J.W., 1988. Genetic interpretations of elemental and chemical differences in a soil chronosequence, California. Geoderma 43, 179–193.
Harden, J.W., Taylor, E.M., Hill, C., Mark, R.K., McFadden, L.D., Reheis, M.C., Sowers, J.M., Wells, S.W., 1991. Rates of soil development from four soil chronosequences in the southern Great Basin. Quaternary Research 35, 383–399.
Hirmas, D.R., 2008. Surface processes, pedology, and soil–landscape modeling of the Southern Fry Mountain Bolson, Mojave Desert, California. Ph.D. dissertation, University of California, Riverside.
Hornbeck, D., 1983. California Patterns: A Geographical and Historical Atlas. Mayfield Publishing Company, Mountain View, CA.
Hubbert, K.R., Graham, R.C., Anderson, M.A., 2001. Soil and weathered bedrock: components of a Jeffrey pine plantation substrate. Soil Science Society of America Journal 65, 1255–1262.
Istok, J.D., Harward, M.E., 1982. Influence of soil moisture on smectite formation in soils derived from serpentinite. Soil Science Society of America Journal 46, 1106–1108.
Johnson, D.L., 1977. The late Quaternary climate of coastal California: evidence for ice age refugium. Quaternary Research 8, 154–179.
Jones, D.P., Graham, R.C., 1993. Water-holding characteristics of weathered granitic rock in chaparral and forest ecosystems. Soil Science Society of America Journal 57, 256–261.
Kendrick, K.J., Graham, R.C., 2004. Pedogenic silica accumulation in chronosequence soils, southern California. Soil Science Society of America Journal 68, 1295–1303.
Le Bissonnais, Y., Singer, M.J., 1993. Seal formation, runoff, and interrill erosion from seventeen California soils. Soil Science Society of America Journal 57, 224–229.
Lee, B.D., Graham, R.C., Laurent, T.E., Amrhein, C., Creasy, R.M., 2001. Spatial distributions of soil chemical conditions in a serpentinitic wetland and surrounding landscape. Soil Science Society of America Journal 65, 1183–1196.
Lee, B.D., Sears, S.K., Graham, R.C., Amrhein, C., Vali, H., 2003. Secondary mineral genesis from chlorite and serpentine in an ultramfic soil toposequence. Soil Science Society of America Journal 67, 1309–1317.
Lee, B.D., Graham, R.C., Laurent, T.E., Amrhein, C., 2004. Pedogenesis in a wetland meadow and surrounding serpentinitic landslide terrain, northern California, USA. Geoderma 118, 303–320.
Marchand, D.E., Allwardt, A., 1981. Late Cenozoic stratigraphic units in northeastern San Joaquin Valley, California. California. U.S. Geological Survey Bulletin 170.
McFadden, L.D., 1982. Impacts of temporal and spatial climatic changes on alluvial soils genesis in southern California. Ph.D. dissertation. University of Arizona, Tucson.
McFadden, L.D., Tinsley, J.C., 1985. Rate and depth of pedogenic-carbonate accumulation in soils: formulation and testing of a compartment model. In: Weide, D.L. (Ed.), Quaternary Soils and Geomorphology of the Southwestern United States. In: Special Paper, vol. 203. Geological Society of America, pp. 23–42.
McFadden, L.D., Wells, S.G., Jercinovich, M.J., 1987. Influences of eolian and pedogenic processes on the origin and evolution of desert pavements. Geology 15, 504–508.
McGahan, D.G., Southard, R.J., Claasen, V.P., 2008. Tectonic inclusions in serpentinitic landscapes contribute plant nutrient calcium. Soil Science Society of America Journal 72, 838–847.
Miller, C.S., Hyslop, R.S., 2000. California: the Geography of Diversity, 2nd ed. Mayfield Publishing Co., Mountain View, CA.
Minnich, R.A., 2007. Climate, paleoclimate and paleovegetation. In: Barbour, M., Keller-Wolf, T., Schoenher, A.A. (Eds.), Terrestrial Vegetation of California. In University of California Press, Berkeley, CA, pp. 43–66.
Merritts, D.J., Chadwick, O.A., Hendricks, D.M., 1991. Rates and processes of soil evolution on uplifted marine terraces, northern California. Geoderma 51, 241–275.
Moody, L.E., 1989. Site and soil characteristics of landslides on soils in San Luis Obispo County, California. M.S. thesis. California Polytechnic State Univ., San Luis Obispo, CA.
Moody, L.E., Graham, R.C., 1994. Pedogenic processes in thick sand deposits on a marine terrace. In: Cremeens, D.L., et al. (Ed.), Whole Regolith Pedology. In: SSSA Special Publication, vol. No. 34. Soil Science Society of America, Madison, WI, pp. 41–55.
Moody, L.E., Graham, R.C., 1995. Geomorphic and pedogenic evolution in coastal sediments, central California. Geoderma 181–201.
Moody, L.E., Graham, R.C., 1997. Silica-cemented terrace edges, central California coast. Soil Science Society of America Journal 61, 1723–1729.
Muhs, D.R., 1982. A soil chronosequence on Quaternary marine terraces, San Clemente Island, California. Geoderma 28, 257–283.
Muhs, D.R., Budahn, J., Reheis, M., Beann, J., Skipp, G., Fisher, E., 2007. Airborne dust transport to the eastern Pacific Ocean off southern California: evidence from San Clemente Island. Journal of Geophysical Research 112, D13203. doi:10.1029/2006JD007577.
Murashkina, M.A., Southard, R.J., Pettygrove, G.S., 2007. Silt and fine sand fractions dominate K fixation in soils derived from granitic alluvium of the San Joaquin Valley, California. Geoderma 141, 283–293.
Nettleton, W.D., Flach, K.W., Borst, G., 1968. A toposequence of soils in a tonalite grus in the southern California Peninsular Range. Soil Surv. Investig. Rep., vol. no. 21. U.S. Gov. Print. Office, Washington, DC.
Nettleton, W.D., Flach, K.W., Nelson, R.E., 1970. Pedogenic weathering of tonalite in southern California. Geoderma 4, 387–402.
Nettleton, W.D., Nelson, R.E., Flach, K.W., 1973. Formation of mica in surface horizons of dryland soils. Soil Science Society of America Journal 37, 473–478.
Norris, R.M., Webb, R.W., 1990. Geology of California. John Wiley & Sons, Inc., New York.
O'Geen, A.T., Hobson, W.A., Dahlgren, R.A., Kelly, D.B., 2008. Evaluations of soil properties and hydric soil indicators for vernal pool catenas in California. Soil Science Society of America Journal 72, 727–740.
Page, A.L., Burge, W.D., Ganje, T.J., Garber, M.J., 1967. Potassium and ammonium fixation by vermiculitic soils. Soil Science Society of America Journal 31, 337–341.
Pevear, D.R., Dethier, D.P., Frank, D., 1982. Clay minerals in the 1980 deposits from Mount St. Helens. Clays and Clay Minerals 30, 241–252.
Pinney, C., Aniku, J., Burke, R., Harden, J., Singer, M., Munster, J., 2002. Soil chemistry and mineralogy of the Santa Cruz coastal terraces. U.S. Geol. Surv. Open-file Report 02–277.
Rains, M.C., Fogg, G.E., Harter, T., Dahlgren, R.A., Williamson, R.J., 2006. The role of perched aquifers in hydrological connectivity and biogeochemical processes in vernal pool landscapes, Central Valley, California. Hydrological Processes 20, 1157–1175.
Rasmussen, C., Torn, M.S., Southard, R.J., 2005. Mineral assemblage and aggregates control carbon dynamics in a California forest. Soil Science Society of America Journal 69, 1711–1721.
Rasmussen, C., Matsuyama, N., Dahlgren, R.A., Southard, R.J., Brauer, N., 2007. Soil genesis and mineral transformation across an environmental gradient on andesitic lahar. Soil Science Society of America Journal 71, 225–237.
Reheis, M.C., 2006. A 16-year record of eolian dust in southern Nevada and California, USA: controls on dust generation and accumulation. Journal of Arid Environments 67, 487–520.
Reheis, M.C., Kihl, R., 1995. Dust deposition in southern Nevada and California, 1984–1989: relations to climate, source area, and source lithology. Journal of Geophysical Research 100, 8893–8918.
Reheis, M.C., Sowers, J., Taylor, E., McFadden, L., Harden, J., 1992. Morphology and genesis of carbonate soils on the Kyle Canyon fan, Nevada, U.S.A. Geoderma 52, 303–342.
Reid, D.A., Graham, R.C., Southard, R.J., Amrhein, C., 1993. Slickspot soil genesis in the Carrizo Plain, California. Soil Science Society of America Journal 57, 162–168.
Rose, K.L., Graham, R.C., Parker, D.R., 2003. Water source utilization by *Pinus jeffreyi* and *Arcotstaphylos patula* on thin soils over bedrock. Oecologia 134, 46–54.
Schwertmann, U., 1993. Relations between iron oxides, soil color, and soil formation. In: Bigham, J.M., Ciolkosz, E.J. (Eds.), Soil color. In: SSSA Special Publication, vol. No. 31. Soil Science Society of America, Madison, WI, pp. 51–69.
Senkayi, A.L., 1977. Clay mineralogy of poorly drained soils developed from serpentinite rocks. Ph.D. dissertation, University of California, Davis.
Singer, A., 2002. Palygorskite and sepiolite. In: Dixon, J.B., Schulz, D.G. (Eds.), Soil Mineralogy with Environmental Applications. In Soil Science Society of America, Madison, WI, pp. 555–583.
Singer, M.J., Bowen, L.H., Verosub, K.L., TenPas, J., 1995. Mössbauer spectroscopic evidence for citrate–bicarbonate–dithionite extraction of maghemite from soils. Clays and Clay Minerals 43, 1–7.
Soil Survey Staff, 1999. Soil Taxonomy, 2nd Ed. USDA-NRCS.
Soil Survey Staff, 2006. Keys to Soil Taxonomy, 10th Ed. USDA-NRCS.
Southard, R.J., Southard, S.B., 1987. Sand-sized kaolinized feldspar pseudomorphs in a California Humult. Soil Science Society of America Journal 51, 1666–1672.

Stam, M., 2004. Soil as significant evidence in a sexual assault/attempted homicide case. In: Pye, K., Croft, D.J. (Eds.), Forensic Geoscience: Principles, Techniques, and Applications. In: Special Publ., vol. 232. Geological Society, London, pp. 295–299.
Strathouse, S.M., 1982. Genesis and mineralogy of soils on an alluvial fan, western Mojave Desert, California. Ph.D. dissertation, University of California, Riverside.
Takahashi, T., Dahlgren, R.A., van Sustern, P., 1993. Clay mineralogy and chemistry of soil formed in volcanic materials in the xeric moisture regime of northern California. Geoderma 59, 131–150.
Tice, K.R., Graham, R.C., Wood, H.B., 1996. Traansformations of 2:1 phyllosilicates in 41-year-old soils under oak and pine. Geoderma 70, 49–62.
Ulery, A.L., Graham, R.C., 1993. Forest fire effects on soil color and texture. Soil Science Society of America Journal 57, 135–140.
Western Regional Climate Center accessed 2008. http://www.wrcc.dri.edu.
White, A.F., Blum, A.E., Schulz, M.S., Bullen, T.D., Harden, J.W., Peterson, M.L., 1996. Chemical weathering rates of a soil chronosequence on granitic alluvium: I. Quantification of mineralogical and surface area changes and calculation of primary silicate reaction rates. Geochimica et Cosmochimica Acta 60, 2533–2550.
White, G.N., Dixon, J.B., 2002. Kaolin–serpentine minerals. In: Dixon, J.B., Schulze, D.G. (Eds.), Soil Mineralogy with Environmental Applications. In Soil Science Society of America, Madison, WI, pp. 389–414.
White, A.F., Schulz, M.S., Vivit, D.V., Blum, A.E., Stonestrom, D.A., Harden, J.W., 2005. Chemical weathering rates of soil chronosequence on granitic alluvium: III. Hydrochemical evolution and contemporary solute fluxes and rates. Geochimica et Cosmochimica Acta 69, 1975–1996.
White, A.F., Schulz, M.S., Vivit, D.V., Blum, A.E., Stonestrom, D.A., Anderson, S.P., 2008. Chemical weathering of a marine terrace chronosequence, Santa Cruz, California I: interpreting rates and controls based on soil concentration-depth profiles. Geochimica et Cosmochimica Acta 72, 36–68.
Wildman, W.E., Jackson, M.L., Whittig, L.D., 1968. Iron-rich montmorillonite formation in soils derived from serpentinite. Soil Science Society of America Journal 32, 787–794.
Witty, J.H., Graham, R.C., Hubbert, K.R., Doolittle, J.A., Wald, J.A., 2003. Contributions of water supply from the weathered bedrock zone to forest soil quality. Geoderma 114, 389–400.
Wood, Y.A., Graham, R.C., Wells, S.G., 2005. Surface control of desert pavement pedologic processes and landscape function, Cima volcanic field, Mojave Desert, California. Catena 59, 205–230.
Young, M.H., McDonald, E.V., Caldwell, T.G., Benner, S.G., Meadows, D.G., 2004. Hydraulic properties of a desert soil chronosequence in the Mojave Desert, USA. Vadose Zone Journal 3, 956–963.
Zelazny, L.W., Calhoun, F.G., 1977. Palygorskite, (attapulgite), sepiolite, talc, pyrophillite, and zeolites. In: Dixon, J.B., Weed, S.B. (Eds.), Minerals in Soil Environments. In Soil Science Society of America, Madison, WI, pp. 435–470.